

## **NOTICE CONCERNING COPYRIGHT RESTRICTIONS**

This document may contain copyrighted materials. These materials have been made available for use in research, teaching, and private study, but may not be used for any commercial purpose. Users may not otherwise copy, reproduce, retransmit, distribute, publish, commercially exploit or otherwise transfer any material.

The copyright law of the United States (Title 17, United States Code) governs the making of photocopies or other reproductions of copyrighted material.

Under certain conditions specified in the law, libraries and archives are authorized to furnish a photocopy or other reproduction. One of these specific conditions is that the photocopy or reproduction is not to be "used for any purpose other than private study, scholarship, or research." If a user makes a request for, or later uses, a photocopy or reproduction for purposes in excess of "fair use," that user may be liable for copyright infringement.

This institution reserves the right to refuse to accept a copying order if, in its judgment, fulfillment of the order would involve violation of copyright law.

## FRACTURING TECHNIQUES AND SOME APPLICATIONS IN ITALY

P. BERRY <sup>1</sup> C. CATALDI <sup>2</sup> E. M. DANTINI <sup>1</sup>

### ABSTRACT

*Problems connected to stimulation processes are analysed as critical parameters that must be taken into account from the research stage through to exploitation.*

*Such an approach is of prime importance for the optimization of the project, for achieving more efficient results during the implementation stage, and finally, for making the best choice of the stimulation technique to be adopted.*

*The relationship between the stimulation treatments and the geo-structural and geomechanical characteristics of the reservoir have been analysed also in the light of some recent experiences in Italy.*

### 1 - INTRODUCTION

For many years now the Oil Industry has been implementing technological operations (stimulation processes) that make it possible to intensify production and to control the exploitation of reservoirs. The way to proceed is decided individually for each case at the end of a drilling program and on the basis of the ensuing results.

The design criteria of the stimulation processes are therefore based on the experience acquired through drillings that do not always turn out to be relevant to the particular case being dealt with. Since, within this context it is not possible to quantify most of the numerous parameters that condition the outcome of the stimulation treatment, the ensuing effects are often disappointing.

A statistical analysis [1] correlating the design data with the results obtained through stimulation can provide the means for a

---

<sup>1</sup> University of Rome

<sup>2</sup> ENEL, National Geothermal Unit

better choice of the method, of the relevant parameters, and furthermore, it can offer a more accurate forecast of the results that can be obtained through stimulation.

The analysis of problems related to the investigation and exploitation of geothermal fields demands an approach making the most of the geostructural characteristics, of the physical and mechanical parameters of the reservoir, and of the complex laws governing its behaviour as concerns the mass and heat flow problems. An appropriate approach should make use of all of these data to solve all the planning and design-related problems.

Indeed, each stimulation generally produces a deep variation in the mechanical and hydraulic characteristics of the surrounding rock mass following an input of energy either in static or in dynamic conditions.

Such processes are however, initially conditioned by the geometry of the hole and by the characteristics of the formation.

As the process gradually spreads out, there are close interactions between the effects of the energy introduced (fractures) and the characteristics of the rock mass, that affect the final outcome of the operation. Keeping account of this close interdependence, the investigation programs for the research and study of geothermal fields should be worked out on the basis of criteria that consider the stimulation techniques as a means of investigation capable of providing useful information on the most important parameters that characterize the reservoir.

Furthermore, the exploitation program should also consider the various solutions provided by the stimulation techniques in relation to the geostructural and geomechanical characteristics of the rock mass.

This paper briefly discusses the problems relating to the correct determination of some of the fundamental parameters that govern the mechanical behaviour of the reservoir rock; the limits of the simplifications usually adopted, will be analysed for the cases in which two of the most widespread stimulation techniques are adopted: hydraulic fracturing and explosive fracturing.

## 2 - BASIC CHARACTERISTICS OF THE ROCK MASS THAT INFLUENCE STIMULATION

In order to optimize any type of intervention in a reservoir it is necessary to have an exhaustive knowledge of the parameters and

laws that govern its behaviour in all the possible situations that could occur.

In particular, during the design and implementation stages, and when analysing the results obtained after stimulation, it is necessary to keep account of the following fundamental parameters.

## 2.1 Original and induced state of stress

In engineering practice, the values and the directions of the three principal stresses are determined by means of well-founded methods that provide both sufficiently accurate data and a reliable interpretation of the results.

As regards Geothermy, attempts to make in situ measurements cannot be made due to the great depths and high temperatures involved. This drawback is usually overcome by assuming that one of the components is vertical and its value is inferred from the density of the formation ( $\gamma$  - logs). Since also this measurement is hampered by the high temperatures of the well, the trend of the values must be extrapolated down to the required depth.

Furthermore, it is virtually impossible to predict the horizontal state of stress merely on the basis of the theoretical considerations. In large areas, experimental measurements have pointed out the presence of higher horizontal stresses than the vertical ones, this being probably due to the tectonic events.

In areas where high temperatures are not involved, the experimental technique based on "hydraulic fracturing" provides useful indications as to the minimal principal stress for wells that are even very deep [2]. The obstacle set up by the high temperatures can be avoided by interrupting the measurements where the temperature starts to be too high, and then the values can be extrapolated down to the required depth.

The results obtained through this technique together with its limits will be analysed in one of the next paragraphs; such results must, however, be interrupted with caution and account must be kept of the mechanical behaviour of the formation.

The original state of stress is deeply modified near the walls of the well. Further variations are due to the static or dynamic pressurization of the borehole (hydraulic or explosive fracturing), or to the mass and heat flow (injection and production).

An analysis of the induced state of stress is rather complex since it is generally characterized by a point distribution of the

principal values and of the principal directions. Furthermore, variations in the hydrostatic stresses exerted by the fluid in the pores (i.e. after an explosion in the blasthole), or the flow that gives rise to hydrodynamic actions in correspondence to the walls of the fractures (i.e. after injections, production or hydraulic fracturing), modify the state of stress.

Experimental results have provided the possibility to check the validity of the law of effective stresses, as far as rocks are concerned, by using the same expression which applies to soft soils. The state of total stress  $\bar{\sigma}$  acting simultaneously with the pore pressure  $P_0$  can be broken down into an effective state of stress and a hydrostatic state of stress, and therefore, the following equation can be written [3] :

$$\bar{\sigma}' = \bar{\sigma} - P_0 \quad (1)$$

## 2.2 Deformability and strength

### 2.2.1 Deformability

The assumption generally made for solving "reservoir engineering" problems (i.e. that rocks are characterized by an isotropic, homogeneous, linear and elastic behaviour) is not true in practice.

Indeed, the mere presence of oriented microfissures causes the rock to show a decidedly anisotropic behaviour. Even for the rocks consisting of minerals having a marked orientation, the anisotropic behaviour is partially to be attributed to the latter, whereas the influence of the microfissures appears to prevail.

The progressive closing of the microfractures brings about evident changes in the linear behaviour (Fig.1) and in the elastic behaviour, and as the stress increases, the deformability tends towards that of the rock matrix, thus entailing a decrease in the anisotropic degree (Fig.2).

When the rock matrix is assumed as being homogeneous and isotropic within the range of investigated pressures, and neglecting the influence of the temperature, the compressibility of the rock matrix  $C_r$  can be taken as constant. The compressibility of the rock  $C_b$  depends not only on the overall volume of the voids but also on the form of the pores (Fig.3) [5,6,7] and it varies with the effective stress [8,9,10].

In particular for some types of rocks, a variation of the  $C_b$  value can be noted both with the direction and with the level of the applied stress [5] that can be ascribed to the closing of the microfissures. At low loads, for rocks such as granite, gneiss, quartzite,

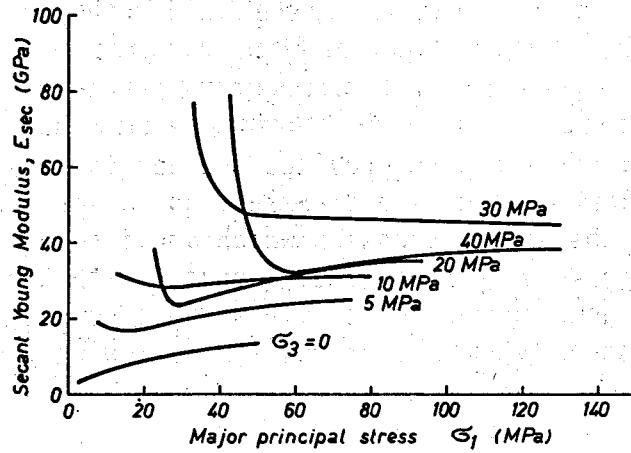


Fig.1 - Secant Young Modulus versus the major principal stress (phyllites from the Larderello field)

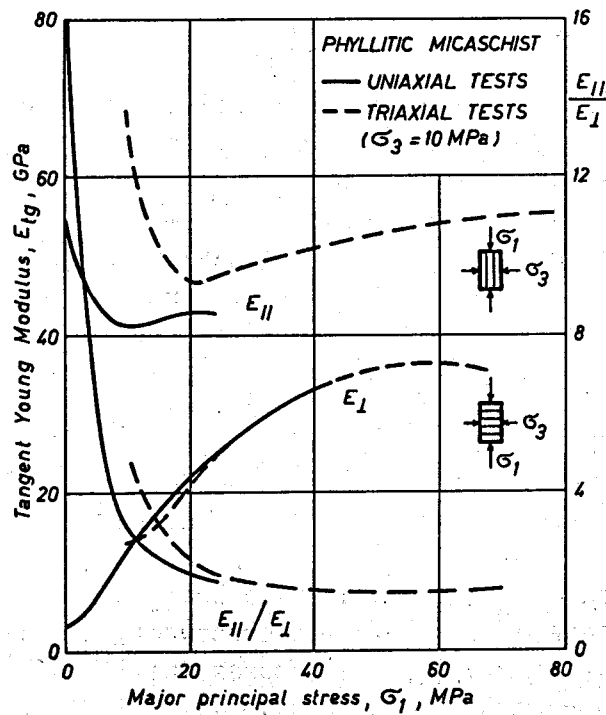


Fig.2 - Tangent Young Modulus versus the major principal stress. At high stresses the deformability of the rock tends to be similar to that of the rock matrix with ensuing decrease in the anisotropy degree [4]

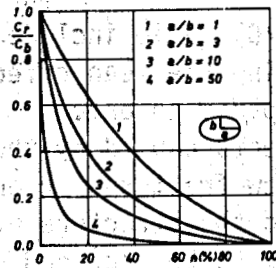


Fig.3 - The compressibility of the rock  $C_p$  depends not only on the overall volume of the voids but also on the form of the pores [7]

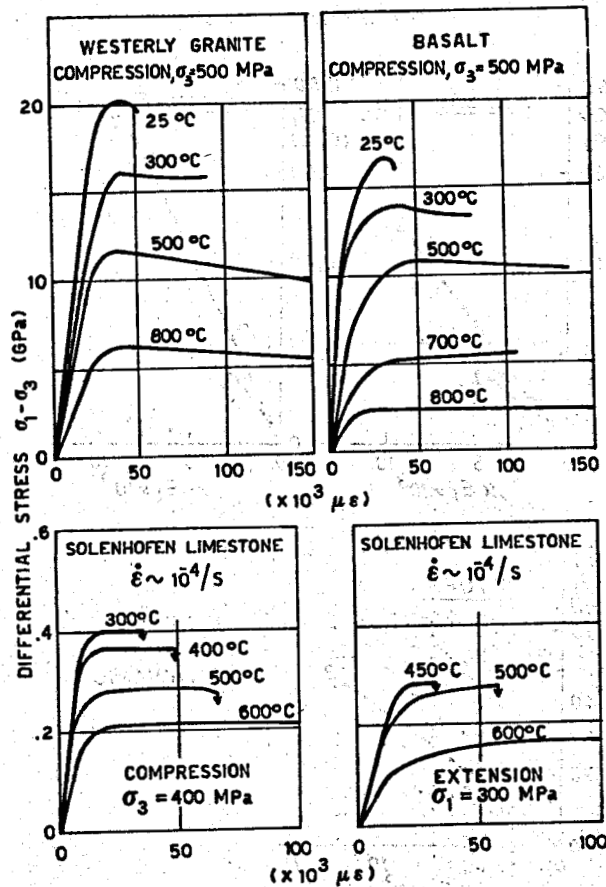


Fig.4 - Stress-strain curves relating to some samples of granite, basalt and limestone for triaxial compression and extension tests. Notice the variation in the mechanical behaviour of the rocks (deformability and strength) when submitted to temperature variations [11]

and marbles, values of the  $C_b/C_r$  ratio included between 7 and 3 were measured, whereas, by increasing the mean effective stress, such values all tend more or less rapidly to one.

If the extent of the effects caused by the temperature variations upon the initiation of new fractures or on the extension of pre-existing discontinuities or on the structure of the composing minerals is changed, the causes are to be ascribed essentially to the type of rock involved and to the way in which the temperature variations are produced.

Laboratory tests [11] have pointed out a progressive increase in the values of the elastic characteristics and a variation of the

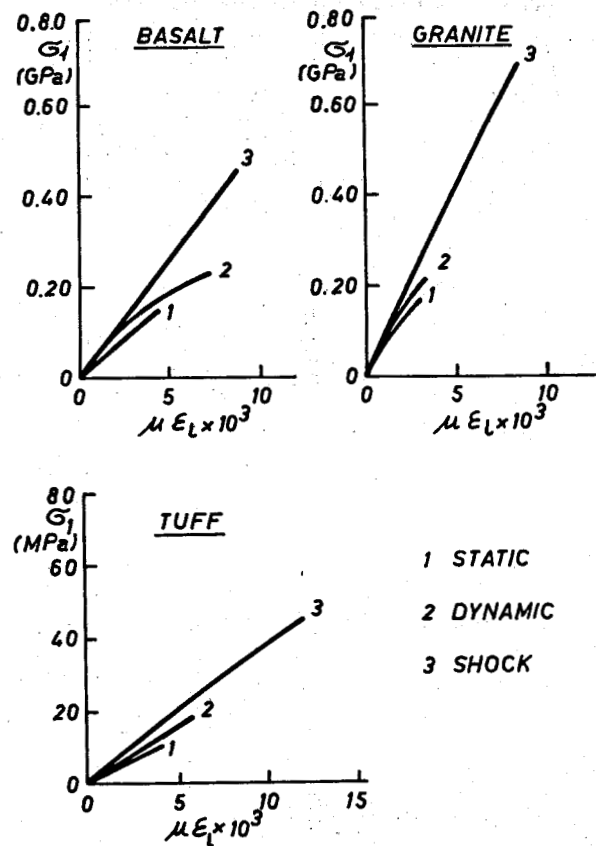


Fig.5 - Stress-strain curves relating to some samples of granite, basalt and tuff for uniaxial compression tests. Notice the variation in the mechanical behaviour of the rock materials (deformability and strength) when they are submitted to different load rates (static, dynamic, shock) [14]



stress-strain curves as the temperature slowly increases (Fig.4).

Also the temperature decrease (due to the injections in geothermal wells) brings about a concentration of stresses caused by the differential deformations of the minerals forming the rock and therefore, a progressive decrease of the stiffness due to thermal cycles is to be expected.

Generally the axial and transversal deformability tends to increase with the load rate depending upon the type of imposed stress and on the characteristics of the rock [12,13]. As regards problems related to explosive stimulations, some laboratory tests provide interesting indications [14] which compare the elastic characteristic of the materials with static and dynamic loads and with shocks (Fig.5).

### 2.2.2 Strength

As previously mentioned even the strength of rocks having brittle behaviour is a function of the effective stresses [15] and in general the strength values grow smaller as the fluid pressure in the microfissures increases.

Even though an adequate number of experimental tests are not available, it may however be assumed that the presence of a fluid in the pores does influence the strength of materials submitted to dynamic stresses produced by explosives. A greater development of the crushed zone and of the radial fractures produced by explosive stimulation is therefore to be expected.

The influence of temperature has been the object of extensive theoretical and experimental research and investigation [11,16] also for stimulation treatments in oil wells [17,18].

With the gradual increase of the temperature values, a considerable decrease in the strength value related to the applied stress can be noticed (Fig.4), and generally the behaviour of the material deeply changes in terms of failure, passing from brittle to perfectly plastic.

The effect of temperature decreases on strength values can turn out to be the same as that noticed for temperature increases. Even in this case rock fracturing is caused by induced stresses in the rock.

The way in which the rock is stressed causes considerable variations in the strength values. In particular when the load rate is close to that obtained by the explosion of a charge in a blast-hole, a considerable strength increase is to be expected (Fig.5).

### 2.3. Flow in continuous porous media

In poorly fractured rock masses having a brittle behaviour and in fractured rock masses (in transitory flow conditions), the motion of the fluid in the matrix which is virtually made possible by the presence of communicating microfissures and pores, becomes considerably important.

The experimental relationships that link the porosity values to the permeability values, as suggested by some authors [19], cannot be applied on a general basis since permeability is a function of many other factors.

Extensive laboratory investigations have pointed out that the pore structure can condition the distribution of the permeability values [20].

Variations in the effective state of stress or in the pore pressure or in the temperature, entail changes in the porosity values.

Fig. 6 shows that porosity decreases as the effective hydrostatic stresses increase for some typical rocks of the Larderello field.

High temperature values cause an extension of the discontinuity network probably because of the differential dilatation of the solid matrix that brings about a concentration of stresses.

For some types of rocks, as temperature increases initially there is a decrease in the porosity, probably caused by the dilatation of the minerals forming the rock. Beyond a certain temperature value, at which new fractures are initiated [12], the porosity gradually increases.

The increase of effective stresses causes the closing of the microfissures and as a consequence a decrease in the permeability values. The extent of such variations depends merely on the form and on the orientation of the pores and microfissures with respect to the applied state of stress and it varies as the latter varies.

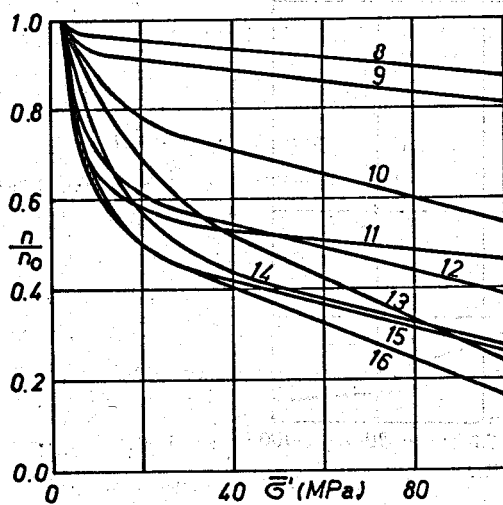
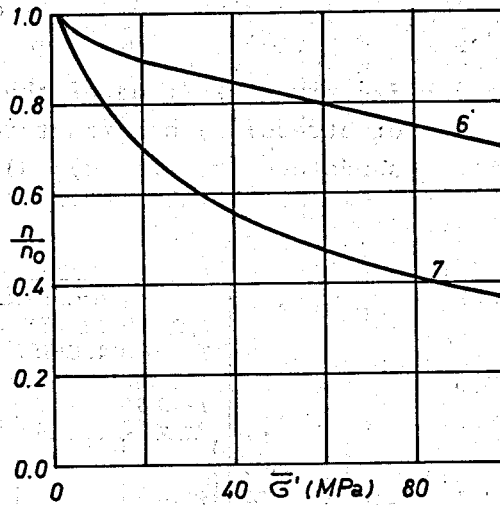
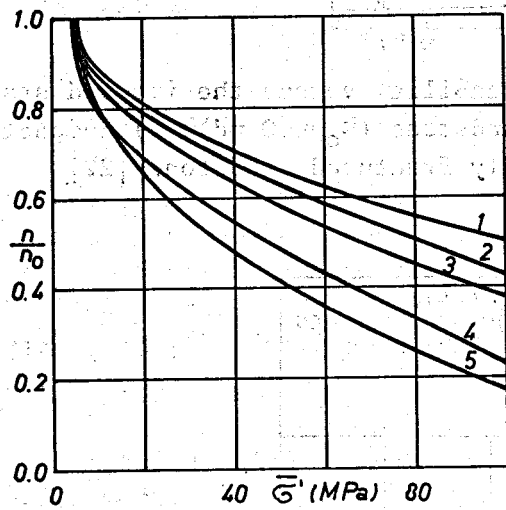
For the case of some sedimentary rocks (Fig.7) that are homogeneous, not fractured and compact with equidimensional pores, permeability generally varies only slightly with the direction and with the intensity of the state of stress [22].

On the other hand for fissured rocks having a rigid behaviour there is a considerable decrease of permeability as the effective stress increases [23, 24] and quite often an anisotropic flow develops.

Fig.8 shows the results of permeability tests performed on

samples of phyllites, recrystallized micaschists and gneiss in the Lardarello reservoir.

Fig. 9 shows the permeability values of the four samples in Fig.8, obtained for different values of the effective hydrostatic stress versus the corresponding differing porosity values. A first analysis has shown that the two parameters appear to be correlated by an exponential law.



LARDERELLO FIELD

POROSITY  $n$  (%) at  $\bar{\sigma}' = 2$  (MPa)

MICASCHISTS

- 1: 1.47
- 2: 1.21
- 3: 1.27
- 4: 0.78
- 5: 0.90

SANDSTONES

- 6: 19.2
- 7: 0.98

PHYLLITES

- 8: 9.15
- 9: 5.99
- 10: 1.38
- 11: 2.91
- 12: 1.75
- 13: 0.88
- 14: 0.64
- 15: 2.04
- 16: 0.76

Fig.6 - Experimental trend of the permeability versus the effective hydrostatic state of stress (Lardarello field)

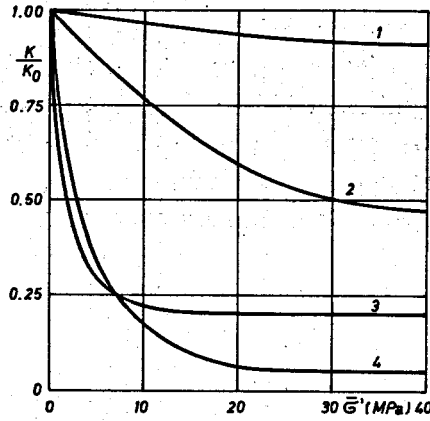


Fig.7 - Experimental trend of the permeability versus the imposed state of stress: 1) non-fractured sandstone ( $k_o = 60$  md); 2) compact sandstone ( $k_o = 25$  md); 3) highly fractured sandstone [22]

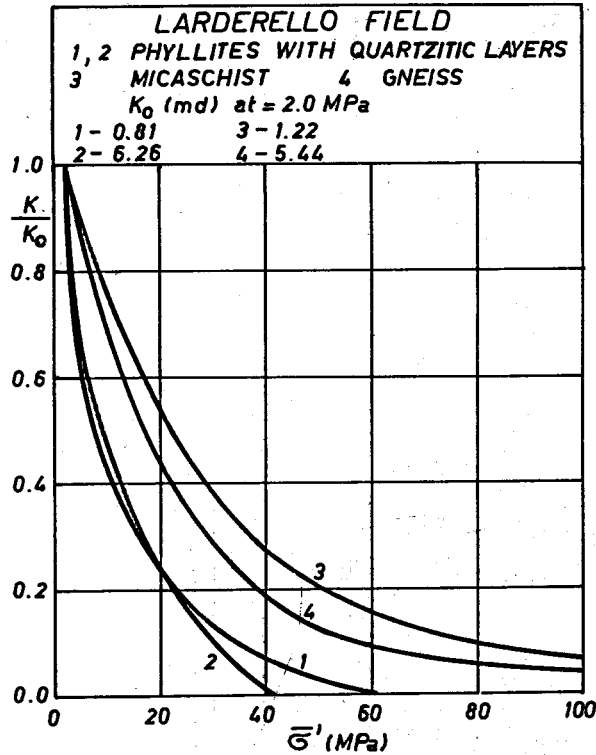


Fig.8 - Experimental trend of the permeability for specimens submitted to hydrostatic effective stresses varying from 2 to 100 MPa (Larderello field)

However, further data are required in order to make a final evaluation as to the general validity of the law.

For rocks having a homogeneous and isotropic hydraulic behaviour, when they are hydrostatically stressed and by assuming that the permeability values depend exclusively on the acting mean effective stress, Morgenstern [26] suggested the following empirical relationship between the permeability and the mean effective stress:

$$k = \frac{A_0}{(\bar{\sigma}' + A_1)^m} \quad (2)$$

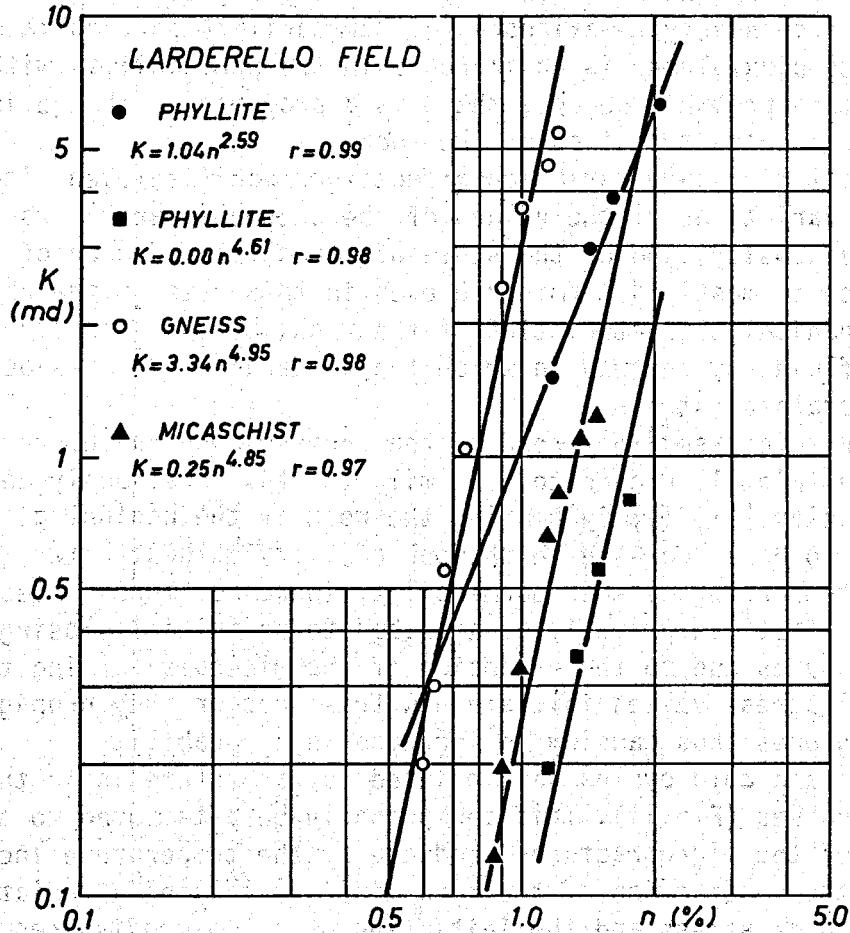


Fig.9 - Relationship between porosity and permeability (Larderello field)

By plotting the permeability values obtained for the samples of the Larderello reservoir in a log-log diagram the curves shown in Fig. 10 are obtained. The trend is a typically curvilinear trend that has been noticed also for other types of rocks having microfissures and a brittle behaviour [23,24,26], and it points out that the values of the coefficients of the empirical relationship depend also on the range of the imposed effective stresses.

Loading and unloading cycles emphasize the irreversible behaviour of the flow [27,28] and this is probably due to the irreversible closing of a part of the microfissures present in the samples.

For very high stress values it is possible to determine the propagation and the coalescence of the microfractures which are emphasized [12] by the rapid increase of the permeability values [29,30].

The dependency relationship of permeability on temperature is rather complex. There is an increase in the permeability with the temperature probably because there is a progressive change in the structural characteristics of the rock.

The temperature variation affects permeability even indirectly through variations of the values of the physical parameters of the fluid (viscosity) and of the state of stress. The degree of the influence is mostly determined even in this case by the physical and mechanical characteristics of the rock, by the characteristics of the fluid, by the way in which the temperature changes occur, and by the state of stress.

For some cases the trend of the permeability values versus temperature (Fig. 11) proved to be similar to that previously described for porosity [21,31]. By heating the rock at the beginning, there appears to be a decrease in the permeability values. Later, for higher temperature values permeability increases more or less rapidly. This fact can probably be ascribed to an initial closing of the microfissures due to the expansion of the minerals forming the rock; critical stress values initiate new fractures or they propagate the existing ones thus causing an increase in permeability.

Hot and cold cycles have pointed out a hysteresis in the permeability values (Fig. 11). This can probably be attributed to the propagation of the microfractures produced by the temperature increase and by the contraction of the rock minerals causing a variation in the state of stress and the initiation of new microfissures.

All the aspects that have been illustrated are made more complex in situ because all the various effects that have been analyzed sepa-

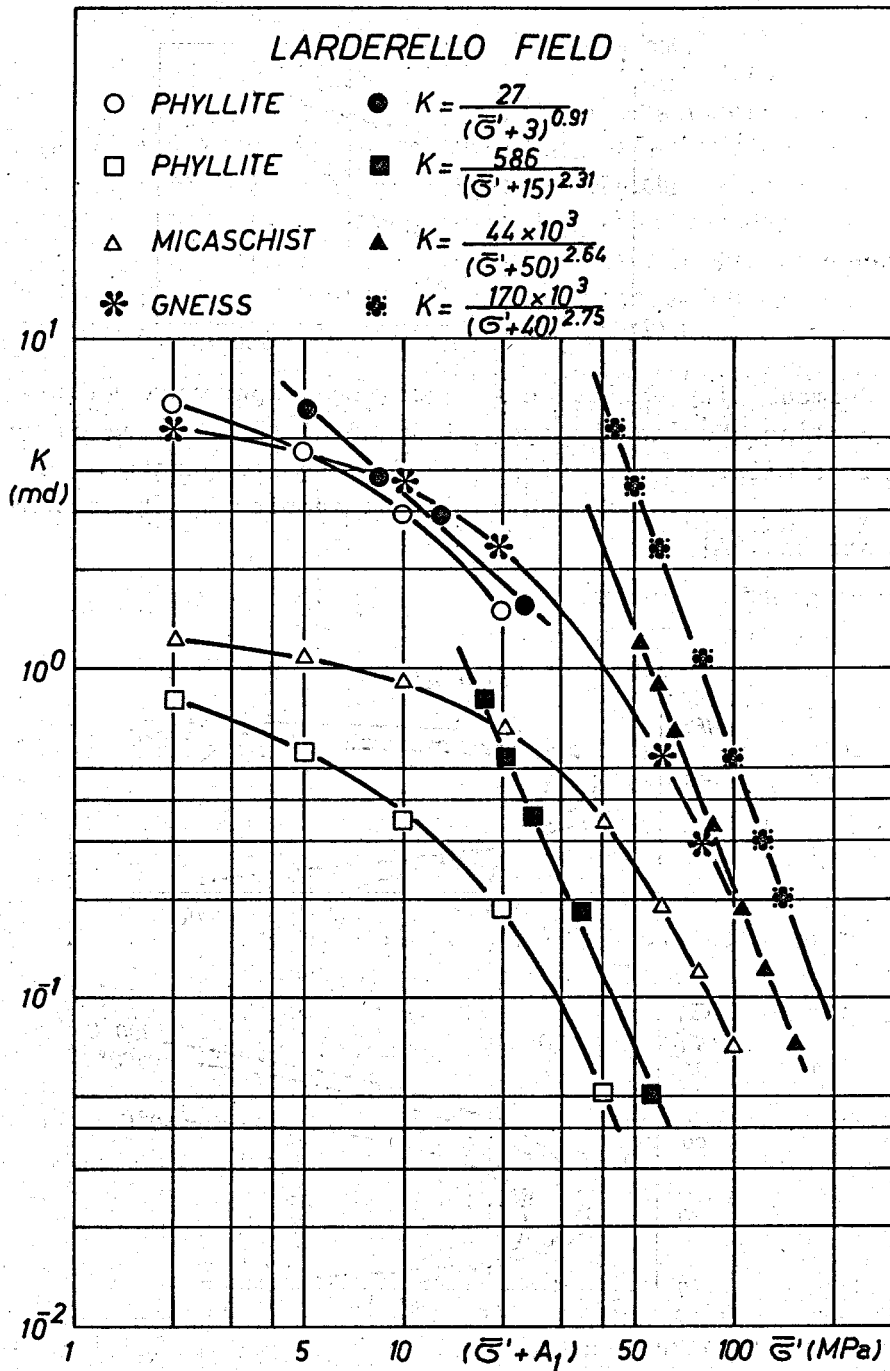


Fig.10 - Experimental trend of the permeability for specimens submitted to hydrostatic effective stresses and experimental data fitted by equation (2) (Larderello field)

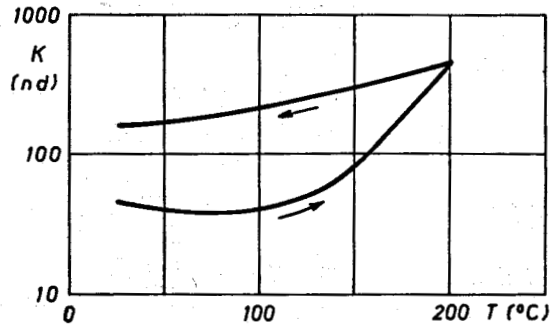


Fig.11 - Permeability variation for growing temperature values and for cooling. Notice the typical trend of the heating curve which is similar to that of porosity versus temperature and the increase in porosity caused in the samples by the thermal stress [24]

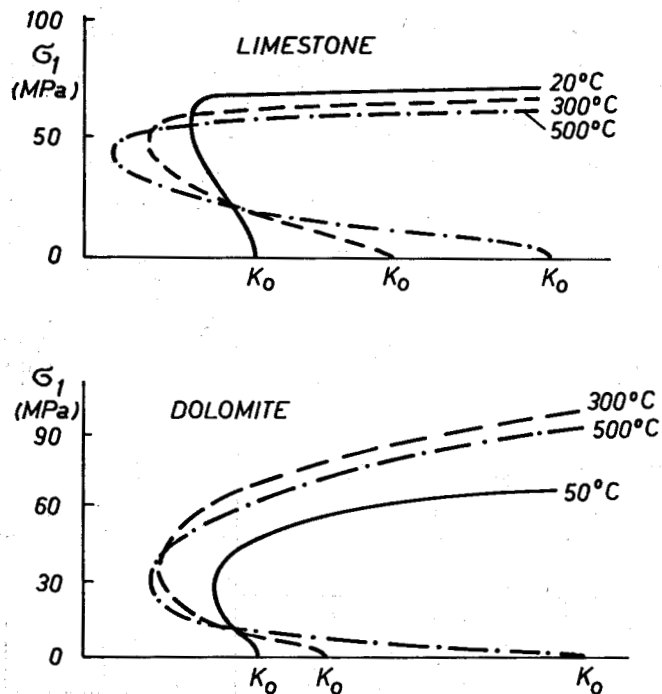


Fig.12 - Permeability variation versus the uniaxial state of stress and the temperature variations. The typical trend is caused by the initial closing of the microfractures and the increase in porosity brought about by the induced stresses [21]



rately obviously overlap.

As an example, Fig. 12 shows the effects on permeability both of the pressure and temperature variations. The curves prove that it is not possible to expect the phenomenon univocally. Indeed, in some cases, temperature appears to play a marginal role as compared with the imposed stress, in other cases thermal stresses have a greater influence. This difference is probably due to the different types of rock and to the type of imposed stress.

## 2.2. Mass flow in fractured rocks

In most geothermal wells the flow under standard conditions occurs through the discontinuities present and is due to the great difference between the permeability values of the rock mass and of the rock material. Some permeability value ranges of a few common rocks are given [32]:

Table 1 : In situ and laboratory permeability values k(cm/s)

ROCK MATERIAL	
Sandstone	$1 \cdot 10^{-10}$ - $2.2 \cdot 10^{-5}$
Granite	$5 \cdot 10^{-11}$ - $2.0 \cdot 10^{-10}$
Limestone and Dolomite	$7 \cdot 10^{-10}$ - $1.2 \cdot 10^{-7}$
ROCK MASS	
Sandstone	$1.0 \cdot 10^{-2}$
Granite	$0.6 \cdot 10^{-3}$
Limestone	$1.0 \cdot 10^{-4}$ - $10^{-2}$
Gneiss	$1.2 \cdot 10^{-3}$ - $1.9 \cdot 10^{-3}$

The following table provides the reservoir formation for some of the most important Italian Geothermal Reservoirs.

The hydraulic characteristics of the fractures condition the flow of the fluid in these reservoirs, and the mechanical behaviour of the rock mass depends mainly on the geomechanical characteristics of the joints.

Experience has shown that in geothermal fields conditions of flow

Table 2 - Italian Geothermal Reservoirs

FIELDS	RESERVOIR FORMATION
Larderello	Quartzites, Phyllites and Anhydrites
Travale	" " "
Monte Amiata	" " "
Piancastagnaio	" " "
Torre Alfina	Limestone
Latera	"
Cesano	"
Lago Patria	Tuffs

anisotropy, dishomogeneity may be found, according to the geometrical characteristics of the fractures (spacing, opening, state of surfaces), to their orientation and distribution, to the extent to which they are filled as brought about by the settling of salts, to the state of stress.

A typical example [32] of dishomogeneous distribution of the flow is found in the Larderello reservoir that represents a reliable means for exploring the details of this problem due to the high number of wells that have been driven.

Another example is the Cesano Reservoir (Fig. 13) where the orientation of the fractures, that are mainly sub-vertical, plays an important role. In the upper part of the reservoir, these fractures are partially closed due to the settling of salts, and besides, intense recrystallization occurs due to the high temperatures. Furthermore, in these reservoirs the inter-section of a high number of discontinuities and their dishomogeneous filling originates canals where the flow runs; these canals could even have led to surface manifestations (volcanic chimneys).

In order to theoretically analyse in a straightforward way the reservoir engineering problems, the rock mass can be schematized as a porous and continuous medium having an anisotropic permeability with, on average, the same characteristics as the real rock mass [33]

In this manner, the value of the average rate can be defined for each point and the proportionality relationship between the velocity vector and the potential gradient vector is defined by means of a symmetric matrix of the permeability [31].

If the objective is that of studying the surrounding of a well inside a reservoir (for example when the well crosses an important dis-

continuity surface or when dealing with stimulation problems), it is preferable to assume a perfectly impermeable continuum crossed by several systems of joints that, more or less, intercommunicate. In this case, the solution to the flow problems can be found by studying in detail, the motion of the fluid through such discontinuities.

Experimental tests [34] carried out on a rough natural fissure in a porphyry specimen in which the joints had different opening conditions, have pointed to a clear non-linear relationship between the flow-rate and the hydraulic gradient. For very low hydraulic gradients

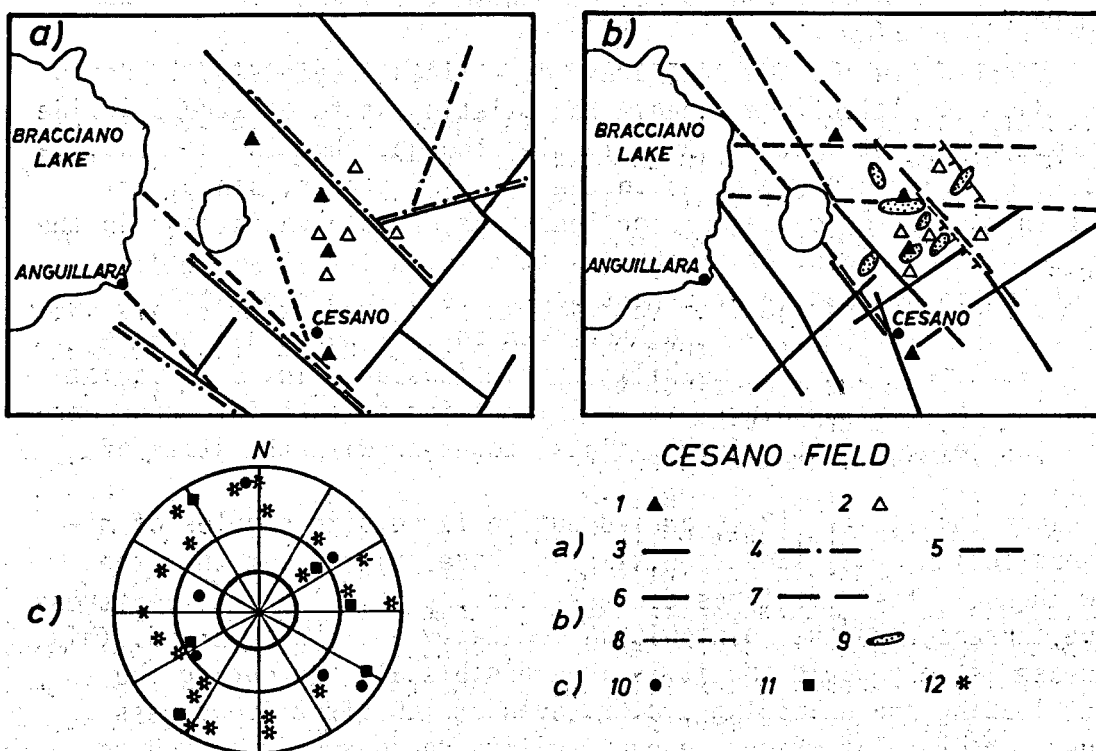


Fig.13 - Structural scheme. Cesano field: a and b show: 1) productive wells; 2) dry wells; 3) electric discontinuities; 4) magnetotelluric discontinuities; 5) gravity anomalies; 6) main regional tectonic lines inferred from photo-geological surveys; 7) alignment of volcanic chimneys; 8) faults; 9) volcanic chimneys Schmidt's net in c shows the directions of the principal faults in outcrops near the Cesano field in the following formations: 9) siliceous limestone ("Corniola"); 10) Dolomite limestone; 11) Limestone ("Calcare massiccio")

there is a progression towards a non-linear laminar condition and finally to a turbulent flow (which is typical in the case of a fracture crossed by a well). On the basis of these results a power law was proposed between the effective mean flow rate of the joint and the opening "e" with an exponent that varies according to the flow rate:

$$q \propto e^m \quad (3)$$

The exponent is 2 for a linear laminar flow; 1.2 for a fully turbulent flow, and it ranges between these two values for the non-linear laminar flow.

Water flow inside the fractures, as noticed previously, leads to hydro-dynamic actions that change the existing state of stress inside the rock mass. It must be borne in mind though, that the permeability inside the fracture depends on the state of stress, since variations in the latter cause more or less considerable variations in the opening of the joints. It is obvious that the water flow problems and of the induced state of stress cannot be solved separately since they mutually influence each other, even in a rather considerable manner at times. Since permeability variations are linked to variations in the joint openings, it is interesting to take into consideration the deformability of the joints, together with the state of stress.

Laboratory tests [27], carried out on large-size samples of micaceous schist or on sandstone samples, have pointed out that the flow through the fractures decreases as the normal effective stress value increases on the joint with a decidedly non-linear trend. This decrease is very rapid and it is irreversible already during the first loading and unloading cycles, even at low effective stress values. The rate at which the permeability decreases is linked to the opening of the fractures. For closed fractures there is a rapid decrease at the low effective stress values, whereas as the stress increases, the permeability value remains constant. For fractures having a larger opening, the constant permeability value is reached at higher imposed effective stress values. Permeability does not markedly vary with parallel stresses at the joints whereas, it decreases considerably and irreversibly with the shear stresses due to dilatation that occurs close to the limit strength conditions of the joint.

Theoretical analyses show that the permeability of the joints varies markedly with the temperature [35]. It must be noted that probably most of the permeability variations must be attributed to the

variations in the state of stress induced by temperature variations.

It must be borne in mind that much caution is necessary when making an evaluation of the hydraulic characteristics of fractures on the basis of results provided by the permeability tests conducted on rock samples because, this evaluation can differ from that inferred on the basis of the in situ measurements. This difference is greater the higher the fracture control on the flow inside the reservoir (as generally occurs in Italian reservoirs).

Indeed, while it is possible to make sufficiently good laboratory simulations of the pressure conditions of the fluid and of the state of stress (when studying the permeability) it is very difficult to obtain a meaningful representation of the fractured medium by using small samples.

Observations made in some fields confirm the fact that permeability and state of stress are mutually interdependent. For the reservoirs where permeability depends almost exclusively on fractures, the decrease in the production of the wells is to be attributed to a decrease in the pressure of the fluid (increase of the effective stress). Conversely, in the reservoirs where matrix permeability prevails, the effective stress appears to have less influence on the latter.

The curves obtained for production and injection tests do not differ much for the reservoirs where matrix permeability prevails, whereas it was pointed out that the injection rate is much higher than the output rate for reservoirs where permeability is due to fractures. Increasing flow values during production lead to an increase in the effective stress that tends to close the fractures. Whereas, for the case of injections, as the flow rate increases the effective stress that acts on the walls of the fractures decreases.

### 3 - HYDRAULIC FRACTURING

As known this technique consists in using a fluid to pressurize a borehole section isolated by packers in order to lead to the failure of the walls of the hole and to a propagation of the fracture. The fracture clearly entails an increase in permeability due to a decrease in the effective stresses.

By analysing the results of "hydraulic fracturing" performed in sandstones and dolomites (Fig. 14) [22] the flow - pressure curves are characterized by three more or less well defined curve portions depending on the permeability characteristics, on the viscosity of the fluid used, and on the injection conditions. The OA interval repre-

sents the initial pressurization of the hole; AB corresponds to the opening of some fractures in the pressurized part of the hole which have a favourable orientation; BC corresponds to the propagation of the preferential fracture.

The curves show a marked linear trend both when very permeable formations are involved (since the fluid can be injected and it is not possible to induce considerable permeability variations in the rock mass) and for formations having an impermeable matrix and scarce structural discontinuities and therefore, the flow is confined to the fracture.

It is possible to make global analyses [22] of the evolution of the permeability of the reservoir versus the effective stresses both during the extraction of the fluid (already discussed previously), and during "hydraulic fracturing" (Fig.15). Figure 15 points out that in

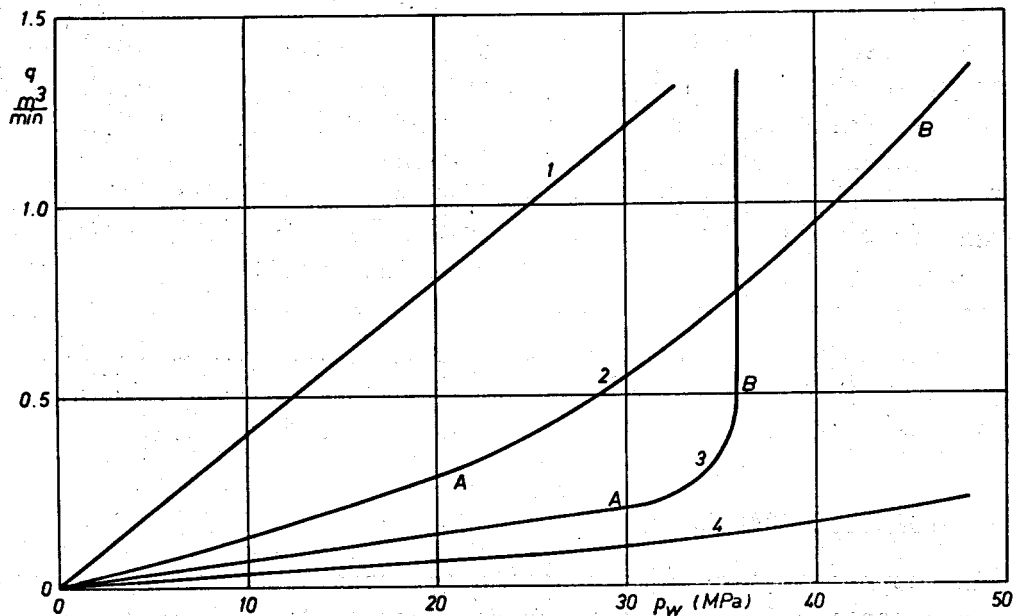
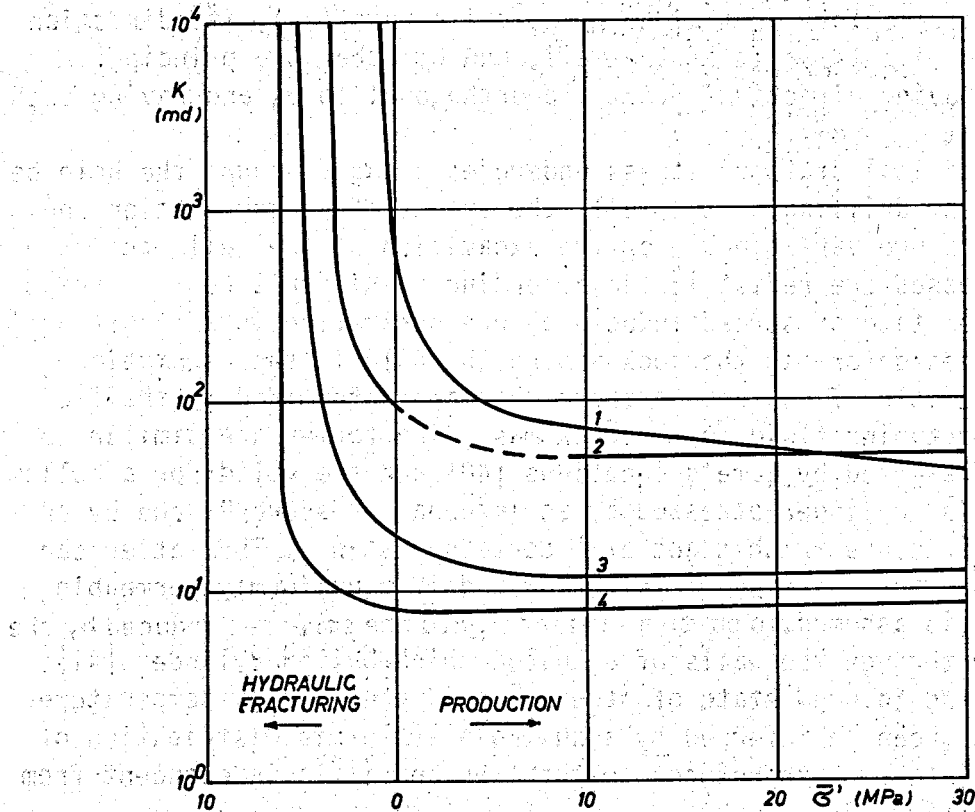


Fig.14 - Hydraulic stimulation in reservoirs having different structural characteristics: 1) permeable sandstone (50-100 md); 2) medium permeability sandstone having slightly permeable fractures (10-50 md); 3) low permeability sandstone (10 md) having very permeable fractures; 4) dolomite reservoirs having very low permeability ( $\ll 1$  md) where a hydraulic fracturing treatment does not cause considerable effects [22]

highly fractured formations the hydraulic fracturing operation merely turns out to be an opening of natural pre-existing fractures. In scarcely fractured reservoirs, the effectiveness of the hydraulic fracturing treatment will depend on the ratio  $(Kh)_{\text{fracture}} / (Kh)_{\text{formation}}$ , that is a function of the initial permeability and of the possibility of keeping the fractures open. Quite obviously, a high ratio can annul the effectiveness of the treatment if the permeability of the formation is close to zero.



**Fig.15 - Permeability versus effective state of stress in hydraulic fracturing.** 1) highly fractured reservoir; 2) slightly fractured, average permeability reservoir; 3) and 4) non-fractured low-permeability reservoirs. It must be pointed out that in highly fractured reservoirs permeability depends greatly on the effective stresses, both during the hydraulic fracturing and during production | 22 |

### 3.1 Fracturing pressure

The induced state of stress around the well and the analysis of the failure phenomena have been dealt with by many authors [36, 37]. The effect of the penetration of the pressurization fluid into the rock has also been recently the object of investigation [38] by assuming that the rock is porous (with fluid in the pores at pressure  $P_0$ ), homogeneous and isotropic and that it has a linearly elastic brittle behaviour. The flow of the fluid caused by the pressurization of the hole at the pressure  $P_w$  follows Darcy's law.

The induced stresses were written for an original state of stress defined by a maximum or minimum principal stress ( $\sigma_3$ ), its direction coinciding with the axis of the well, and by other two principal stresses having directions that are orthogonal to  $\sigma_3$  and having such values that  $\sigma_{H1} > \sigma_{H2}$ .

The original state of stress undergoes changes around the hole because of the drilling of the well, the effect of pressurization and the temperature variations. For the excavation of the well, the original stresses are redistributed according to Kirsch's relationships [40]. The state of stress induced by pressurization is a result of the stresses deforming the rock around the hole in the assumption that there is no flow, and of those that are determined by the flow of the fracturing fluid in the rock mass. The former are similar to those represented by Lamé's equations [40] and are valid for a hollow thick-walled cylinder stressed by an internal pressure  $P_w$  and by an external pressure  $P_0$  that act at a certain distance. The latter can be obtained for an axi-symmetric flow and if a uniformly permeable formation is assumed, in quite a similar way to the stresses induced by the heat flow through the walls of a hollow thick-walled cylinder [41]. Finally, the induced state of stress around the hole by temperature variations, can be inferred by assuming a symmetric distribution of the temperatures with respect to the axes and it is independent from the depth [40, 42].

By overlapping all of these effects, the following relationships are obtained that give the effective radial, tangential and axial stresses to the walls of the well:

$$\sigma'_v = 0 \quad (4)$$

$$\sigma'_\theta = \sigma'_{H1} (1 - 2\cos 2\theta) + \sigma'_{H2} (1 + 2\cos 2\theta) - p_w \left( 2 - \alpha \frac{1 - 2\nu}{1 - \nu} \right) + \frac{\beta E \Delta T}{1 - \nu} \quad (5)$$



$$\sigma'_z = \sigma'_v - 2\nu (\sigma'_{H_1} - \sigma'_{H_2}) \cos 2\theta - p_w (1 - \alpha \frac{1-2\nu}{1-\nu}) + \frac{\beta E \Delta T}{1-\nu} \quad (6)$$

In these relationships the overpressure that determines the flow is provided by:

$$p_w = P_w - P_o \quad (7)$$

where  $\nu$  is Poisson's coefficient that in most cases takes on values from 0.2 to 0.3;  $\alpha$  is a parameter that keeps account of the mechanical response of the rock in relation to the flow [8,41,42]. It is expressed by:

$$\alpha = 1 - \frac{C_r}{C_b} \quad (8)$$

and it can be determined by laboratory tests [9].

On the basis of the foregoing it can be stated that microfissures bring about a clearly non-linear behaviour, especially at low pressures where the  $\alpha$  values for the most common rocks range from 0.9 to 0.7, whereas, as the effective stresses increase,  $\alpha$  tends to values ranging between 0.04 and 0.06.

The relationships point out that as overpressures  $P_w$  increase, the axial and tangential stresses tend to become tensile stresses. The minimum value of a pressure necessary for inducing tensile stresses along the walls of the well is obtained when  $\theta = 0$  and so the relationships are as follows:

$$\sigma'_\theta = 3\sigma'_{H_2} - \sigma'_{H_1} - P_w (2 - \alpha \frac{1-2\nu}{1-\nu}) + \frac{\beta E \Delta T}{1-\nu} \quad (9)$$

$$\sigma'_z = \sigma'_v - 2\nu (\sigma'_{H_1} - \sigma'_{H_2}) - P_w (1 - \alpha \frac{1-2\nu}{1-\nu}) + \frac{\beta E \Delta T}{1-\nu} \quad (10)$$

So, one might conclude that if, as often occurs in practice,  $\sigma'_v$  is the maximum principal stress or, if it is the minimum principal stress, but the difference  $(\sigma'_{H_1} - \sigma'_{H_2})$  is not very high, a vertical fracture will be induced along the  $H_2$  wall of the well.

The limit value of the pressure at which failure occurs is expressed by the following relationship:

$$P_w^c = \frac{\sigma'_t + 3\sigma'_{H_2} - \sigma'_{H_1} + \beta E \Delta T / (1-\nu)}{2 - \alpha (1 - 2\nu / 1 - \nu)} \quad (11)$$

where if the  $\nu$  and  $\alpha$  values are as previously indicated, the denominator generally ranges between the limits:

$$1.3 \leq 2 - \alpha \frac{1-2\nu}{1-\nu} \leq 1.9 \quad (12)$$

and for the same rock it varies as the pressure varies. The lower limit can be applied for impermeable rocks, whereas the upper limit can be applied for permeable rocks.

Relationship (11) points out that the distribution law of the pressures, as determined by the injected fluid, does not influence the state of stress in correspondence to the walls of the well, and therefore it does not affect the value of the fracturing pressure. Vice versa, the experimental results (Fig.16) obtained in the laboratory [44,45] and in situ [46], have pointed out that the strength values obtained by controlling the rate of pressurization, are different from those obtained by controlling the value of the flow. Whereas, by means of the latter procedure, the increment rate of the load does not affect the strength, in the former case the strength increases as

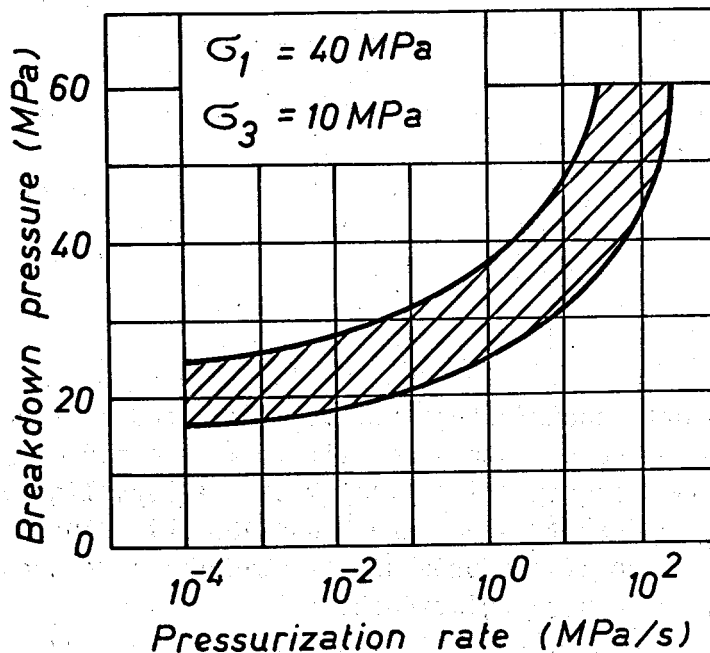


Fig.16 - Hydraulic fracturing: influence of the pressurization rate on the strength of the rock samples [44]

the rate increases, as one might expect. This must probably be attributed to the greater probability of failure occurring as the rock volume increases around the pressurized hole interval. Indeed, experimental measurements have shown that strength decreases even as the diameter of the pressurized interval increases [45].

Laboratory results [47] show that for scarcely permeable rocks, the value of the breakdown pressure versus the confining horizontal pressure differs considerably from the linear trend expected by expression (11). In particular, for increasing values of  $\sigma_H$ , the values of  $p_W^C$  tend to decrease progressively down to the critical values obtained for permeable rocks (lower limit of relationship (12)). This trend could correspond to a permeability increase as previously discussed, brought about by high stresses, that allow a higher penetration of the fluid. Indeed, it must be borne in mind that, at the beginning, the denominator of the relationship assumes a value that is close to one when the load values are zero, whereas, it tends to the typical maximum limit of scarcely permeable rocks as the stresses increase.

The experimental analysis has pointed out that anisotropy has a high influence [48] on the  $p_W^C$  values. Under the same confining stresses where  $\sigma_V > \sigma_H$  and independently from the  $\sigma_V / \sigma_H$  ratio, the  $p_W^C$  values are higher when the injection hole is orthogonal to the schistosity planes and it gradually decreases down to the minimum value when schistosity is parallel to the axis of the well.

If the hole is crossed by joints, the values of the breakdown pressures can prove to be independent from the tensile strength of the rock  $\sigma_t$ . This independence is a function of the geometrical and hydraulic characteristics of the fracture, of the state of stress and of the pressurization methods, as already described. According to the foregoing paragraph, in these cases, the fluid merely flows through pre-existing fractures, and it enlarges them.

A typical example is provided by Fig. 17, which relates to an acidifying process carried out in the Torre Alfina Reservoir [49]. It can be noticed that during the first instance the pressure increases with the flow (in order to reach a pressure value of about 16 MPa, a flow of about 40 m<sup>3</sup>/h is necessary), subsequently, the pressure increases up to 18 MPa and fluid is injected for a constant flow; the rapid and irregular decrease of the pressure values would represent the interconnection of the pre-existing fractures. The subsequent increase of the flow up to about 90 m<sup>3</sup>/h is not sufficient to raise the pressure to the maximum values and furthermore, even though the flow

is maintained around this value, there is a corresponding progressive and irregular decrease of the pressure. The latter pressure decrease is probably related to the pressure increase measured inside the annulus between the casing and the drill pipes, determined by the extension of the rock volume involved in the fracturing treatment. Indeed, it is quite probable that treatment has also affected the walls of the open hole beyond the packers.

The volume of the rock mass affected by the fracturing processes increases during the second phase of the stimulation treatment. In fact, from the very first instant, the pressure in the annulus increases regularly with the flow. Subsequently, with a considerable flow increase the annulus pressure decreases down to values close to zero and this seems to indicate that the open hole is connected with a wider zone of the rock mass.

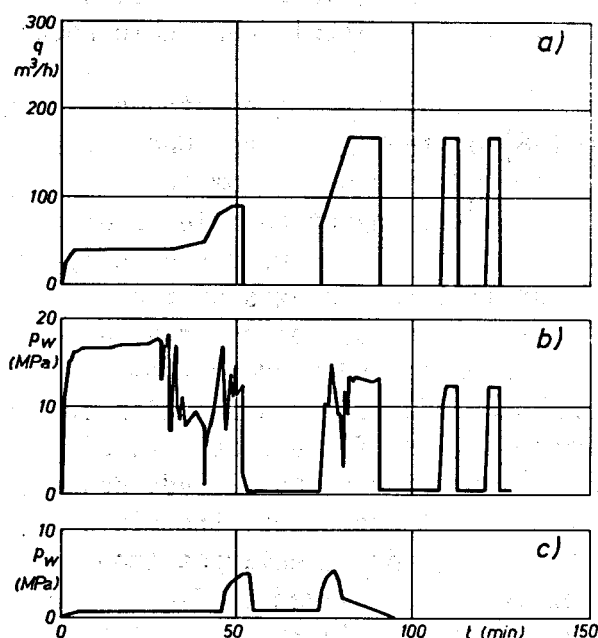


Fig.17 - Hydraulic stimulation at the Torre Alfina well: a) flow versus time; b) pressure in the pressurized interval measured at well head versus time; c) pressure in the annulus measured at well head versus time. The three diagrams relate to the phases: 1) injection of about  $10 m^3$  of water solution containing about 4% HCl; 2) injection of  $40 m^3$  of the water solution containing 15% HCl; 3) and 4) injections of  $12 m^3$  of water each

a wider zone of the rock mass.

During the last two phases, when the flow exceeds 150 m<sup>3</sup>/h, the pressure values are slightly over 12 MPa at the well head and no overpressure is noticed inside the open hole.

### 3.2 Orientation, propagation and geometry of the induced fractures

Under the simplifying assumptions made, the induced fracture should have a vertical direction. Laboratory and in situ tests have pointed out that even horizontal or inclined fractures can be induced because of the inevitable irregularities that are present in the walls of the pressurized interval [46]. The probability of obtaining horizontal fractures increases when one of the ends of the pressurized interval is the bottom of the well. In this case the horizontal fractures are helped by the concentration of stresses linked to the geometry of the well bottom. Similarly, horizontal or inclined fractures can be initiated near rigid packers due to the high value of the vertical tensile stresses [37] which is clearly greater than that of the tangential stresses, whereas, the utilization of rubber packers maintains higher tangential stress values than the vertical ones along the entire length of the pressurized interval.

Fractures having an anomalous direction as compared with those to be expected on the basis of the foregoing theory, for ideal material, should generally deviate at a distance from the walls of the hole, down to the vertical direction. In particular for the case in which a pre-existing fracture were to cross the well, according to the theory based on the concepts of "Fracture Mechanics", for a non hydrostatic principal state of stress, the propagation of a fracture inside a medium having a linear elastic behaviour follows a route in which the deformation energy density assumes a minimum value. Therefore as it lengthens, the pre-existing fracture tends to assume an orientation that is perpendicular to the minimum principal stress [50]. It must be pointed out that the state of stress induced around the edges of the fractures produces a concentration of stresses that aim at plasticizing a part of the rock. Furthermore, the fractures that are present at a distance from the hole having appropriate geometric characteristics could sensitively deviate the propagating fracture (Fig.18), that would thus assume a configuration that virtually could not be predicted.

The calculation methods for the propagation and geometry of the fractures induced by hydraulic fracturing are all based on the

assumption that the rock is homogeneous, isotropic and characterized by an elastic behaviour.

Two fundamental calculation techniques were developed: one keeps account of the mechanical characteristics of the rock that is assumed to be impermeable [51], the other method keeps account of the flow through the walls [52]. An overall analysis of the various methods allows an evaluation of the geometrical parameters of the fractures as the various fundamental parameters involved vary [53].

According to such theories, an induced vertical fracture is a

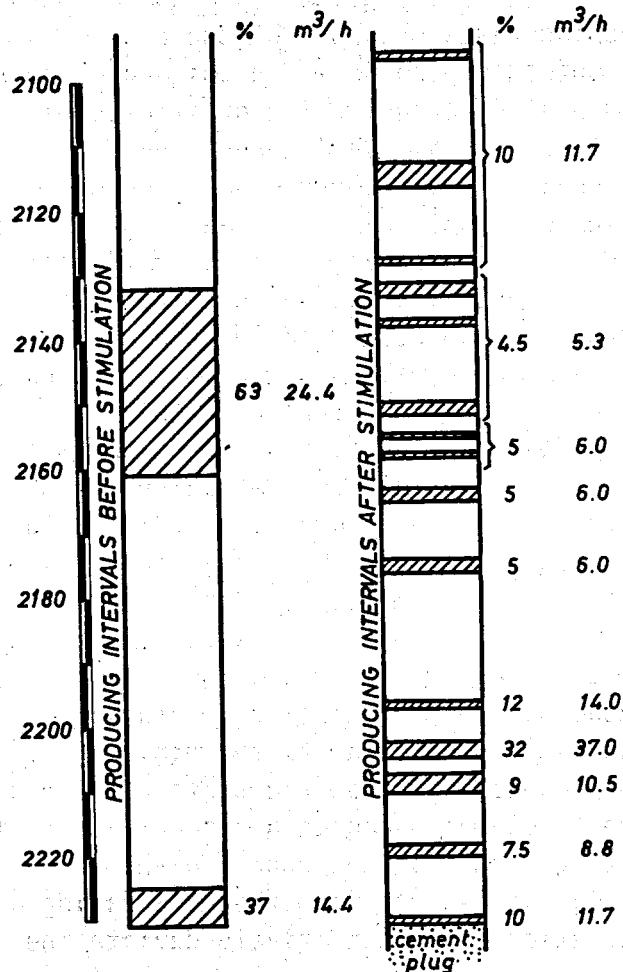


Fig.18 - Hydraulic stimulation at the Torre Alfina well. The Figure points out the height of the formation near the well involved in the stimulation and the opening and connection of pre-existing fractures

few millimeters wide and can propagate for several hundreds of metres. It is obvious that these results derive from the solution of mathematical models that do not keep account of the actual geological and structural complexities, and of the laws that govern its actual mechanical behaviour. The flow and the mutual influence between flow and state of stress.

#### 4 - CHEMICAL EXPLOSIVE STIMULATION

##### 4.1 - Propagation of the crushed zone and of the radial fractures

The system of fractures induced by a "camouflet explosion" and their propagation are conditioned by the characteristic parameters of the explosive and of the rock mass, by the geometry of the explosive and by the decoupling.

The maximum extension of the crushed zone and of the radial cracking zone that can be obtained in homogeneous and isotropic rock masses can be calculated by [54]:

crushed zone	spherical	$\phi_{cr} = A_2 W^{1/3}$	(13)
--------------	-----------	---------------------------	------

	cylindrical	$\phi_{cr} = A_3 Q^{0.5}$	(14)
--	-------------	---------------------------	------

radial cracking zone	spherical	$\phi_r = 1.6 A_4 W^{1/3} (0.48 B_c^{0.5} + 1)$	(15)
----------------------	-----------	---	------

	cylindrical	$\phi_r = 2.5 A_5 Q^{0.5} (0.32 B_c^{0.67} + 1)$	(16)
--	-------------	--	------

The coefficients  $A_2$  and  $A_3$  can be estimated on the basis of the relationship between the extension of the crushed zone versus the characteristic impedance of the rock (Fig.19). The coefficient  $A_4$  and  $A_5$  are respectively equal to 0.24 and 0.11 for rocks having the same characteristics as the Lithonia Granite and for an explosive having a mean detonation velocity.

Relationships have been worked out [55] on the basis of the results obtained with nuclear explosives:

the simplified assumption that the result of the explosion is independent from the mechanical characteristics of the rock mass. Furthermore, it must be pointed out that there is only a slight difference between these coefficients and those obtained with the results of conventional explosions in spite of the fact that the quantity used is many orders of magnitude smaller than the nuclear explosives.

Figure 20 shows the empirical relationships proposed [56] on the basis of the experimental results provided by explosions of conventional spherical charges. However, the trend proposed, appears to disagree with the physical and mechanical phenomena that govern the fracturing processes. With reference to the maximum experimental values, the coefficients of the relationships indicating the extension of the crushed zone are obtained:

$$\phi_{cr} = 0.47 W^{1/3} \quad (19)$$

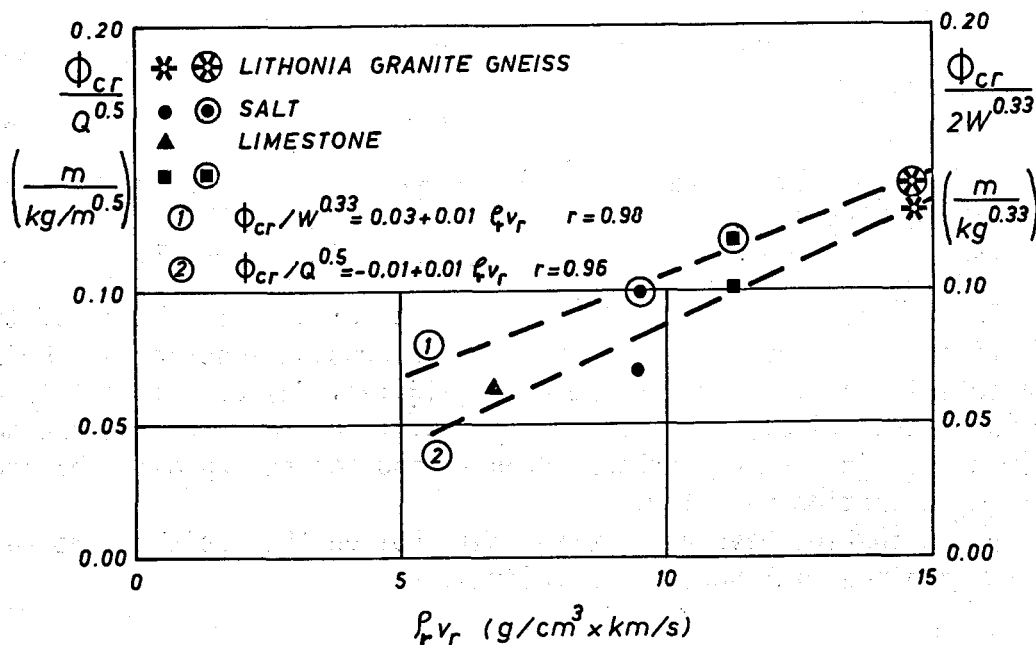


Fig.19 - Influence of the mechanical characteristics of the rock on the extension of the crushed zone. The analysis was carried out for spherical and cylindrical charges. The values shown represent the average of the results obtained by using various types of explosive [54]



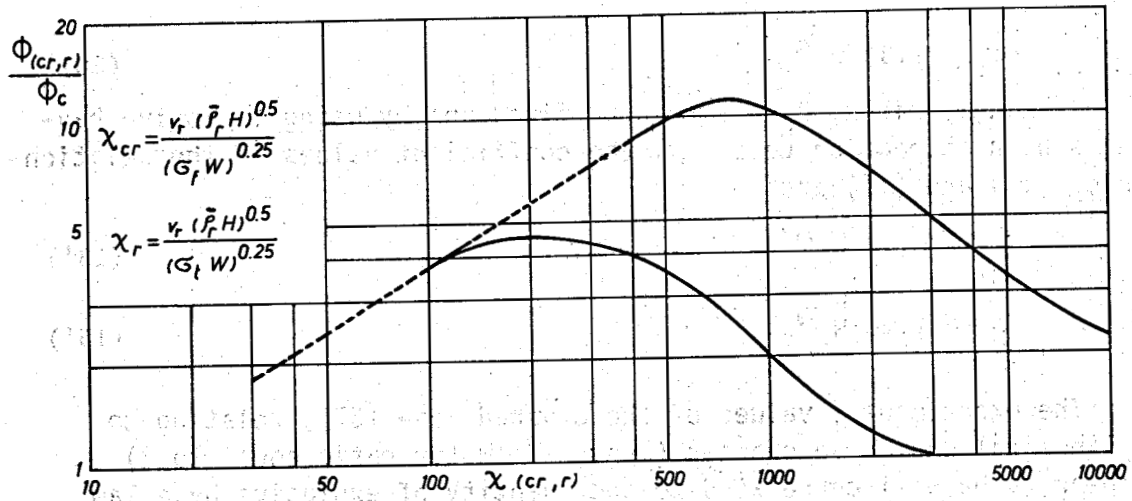


Fig.20-Extension of the radial crack (upper curve) and of the crushed zone versus adimensional groups that keep account of the characteristics of the explosive, of the rock and of the vertical state of stress [56]

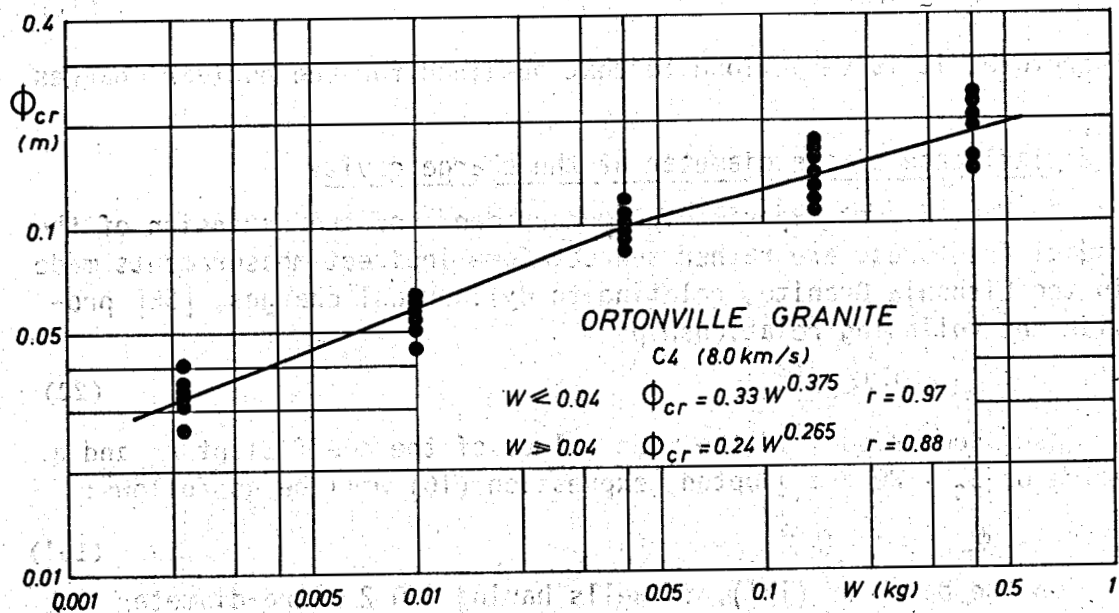


Fig.21-Extension of the crushed zone versus the quantity of explosive. The correlation analysis is based on the experimental results obtained through the explosion of cylindrical charges (the height-diam. ratio being equal to 2) [57]

$$\phi_r = 1.36 W^{1/3} \quad (20)$$

As a comparison,  $B_c = 20$  can be fixed and by using explosive having a high detonation velocity, the coefficient values of the relationships (13) and (15) are:

$$\phi_{cr} = 0.28 W^{1/3} \quad (13')$$

$$\phi_r = 1.20 W^{1/3} \quad (15')$$

The experimental values of the crushed zone [57], relating to cylindrical explosive charges (length-diameter ratio equal to 2) appear to be well correlated to the quantity of explosive by a law of the bilinear type (Fig.21). This result appears to suggest the variability of the coefficients and of the exponents of the relationships used to evaluate the extension of the crushed zone.

By carrying out a correlation analysis of the linear type and by imposing that the geometry of the explosive charge must be spherical, the value of the coefficient is:

$$\phi_{cr} = 0.24 W^{1/3} \quad (21)$$

therefore, it is very close to that obtained for the nuclear charges.

#### 4.2 Influence of the diameter of the charge cavity

So far, direct experimental measurements of the extension of the radial fractures, are rather scarce. Some indirect measurements made in the Lithonia Granite, relating to cylindrical charges, [58] provide the following relationship:

$$\phi_r = 0.37 Q^{0.5} \quad (22)$$

As a comparison, if the mean values of the coefficient  $A_5$  and a value of  $B_c = 20$  are adopted, expression (16) will be as follows:

$$\phi_r = 1.0 Q^{0.5} \quad (16')$$

On the basis of (16'), in wells having a 0.2 metre-diameter and by assuming a charge density of  $1.4 \text{ kg/dm}^3$ , the radial cracking zone would extend to a diameter of 7 metres.

The development of the radial cracks and of the crushed zone increases linearly, the charges being the same, as the diameter of the

hole increases. A calculation example is given in Fig. 22 where (14) and (16') were used and a charge density of  $1.4 \text{ kg/dm}^3$  and a mean value of coefficient  $A_5$  were considered. This example suggests that in a homogeneous material having appropriate mechanical characteristics it is possible to obtain a greater extension of the crushed zone by means of a succession of explosions in the same well, each utilizing the crushed zone of the previous explosion as charge cavity. The upper limit of the extension is obviously conditioned by the technical problems involved in removing the rubble that obstructs the new charge cavity.

Figs. 23, 24 and 25 show an example of the size of the new volumes that can be used as charge cavities. The calculation was made by analysing the experimental results obtained [59,60] through single and multiple explosions performed in rocks having different mechanical and physical characteristics; explosives having varying "power" were used and the charges were spherical.

The different influence of the type of rock and of the type of explosive on the extension of the crushed zone emerges clearly. Indeed, while in the salt and limestone the extension of the crushed zone does not depend on the type of explosive used, in granite the latter is critical [54]. However, as to granite, this dependence tends to decrease in the explosions following the first one; this might probably be due to the drop in the peak and residual values of the mechanical characteristics of the medium, at the radial cracking zone.

As a preliminary indication, it must be pointed out that the tests carried out in the same rock [61] with explosives having different characteristics and decoupling varying between 1.2 and 1.26, seem to show that the extension of the crushed zone is independent from the type of explosive used if decoupling is kept greater than one (Fig.26).

Expression (16) provides an evaluation of the extension of the radial cracking brought about by a succession of explosions in the same hole, but the volume of the charge cavity increases progressively. Under the assumption that the sequence of explosions does not initiate new fractures but merely propagates the existing ones induced by the previous explosions, expression (16) will thus read:

$$\phi_r^{(N)} = 2.5 A_5 Q^{0.5} \left[ 1 + 0.37 \frac{B}{C}^{0.67} + \sum_{a=1}^N (A_5 N)^{a-1} \right] \quad (16'')$$

The evolution of radial cracks according to (16'') for explosions

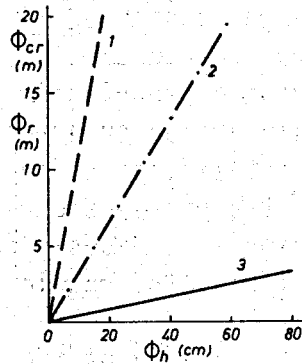


Fig.22 - Extension of the crushed zone (curve 3) and of the radial cracks (curve 2) in the rock mass which is similar to the Lithonia Granite, versus the diam. of the hole. The values are based on explosions where decoupling was equal to 1. Curve 1 provides the extension of the radial fractures in the presence of discontinuities.

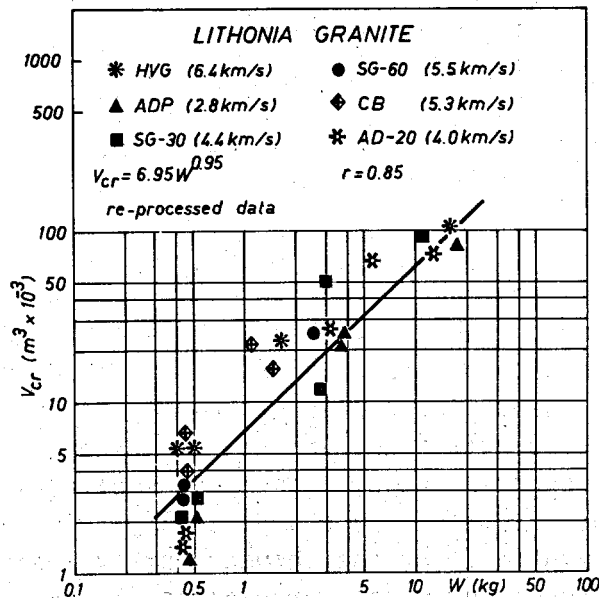


Fig.23 - Correlation and analysis between the extension of the crushed zone and the quantity of explosive. The values analysed are based on multiple successive explosions performed in the same blasthole. As regards the first explosions the marked influence of the type of explosive on the extension of the crushed zone must be noticed. This influence appears to decrease for the explosions following the first one [60]

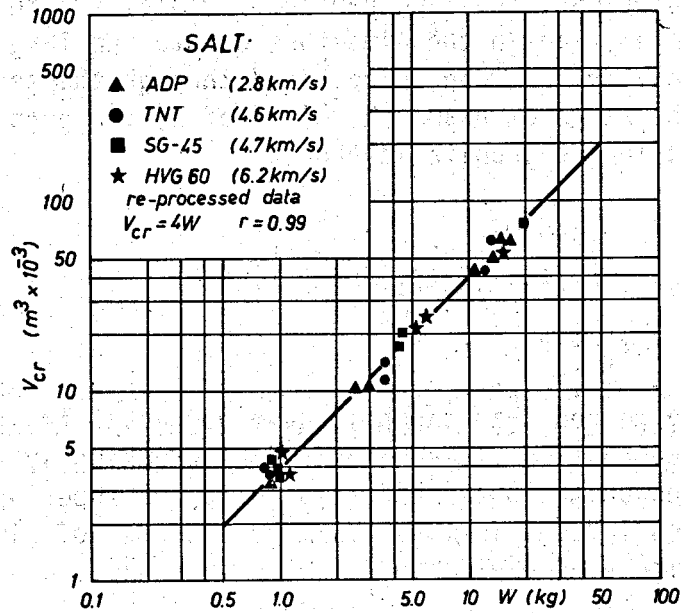


Fig.24 - Correlation analysis between the extension of the crushed zone and the quantity of explosive. The values are based on multiple successive explosions performed in the same borehole. In this rock mass the extension of the crushed zone is not influenced by the type of explosive used [59]

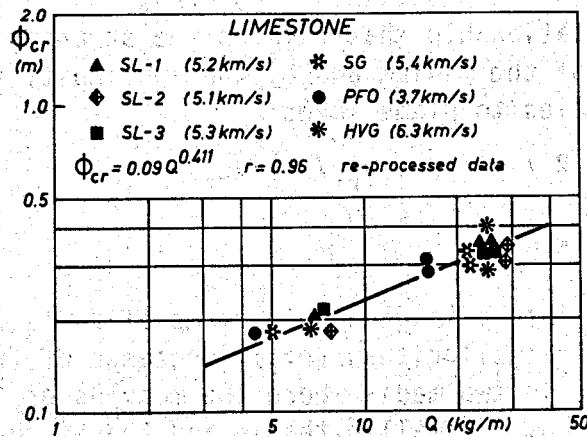


Fig.25 - Extension of the crushed zone versus the quantity of explosive contained in a 1-m hole. For this rock material the diameter is not influenced by the explosive used

in granite rocks and limestone [62] is shown in Fig. 27 versus the number  $N$  of explosions. The lengthening of radial fractures in the granite is greater than in the limestone due to the larger volumes of the charge cavity that can be obtained through the sequence of explosions. In the range of examined values of  $N$ , the propagation that can be obtained in the granite is about:

$$\phi_r^{(N)} / \phi_r = 5 \quad (23)$$

whereas for the limestone it is:

$$\phi_r^{(N)} / \phi_r = 2 \quad (24)$$

A different method that can help develop radial fractures and guarantee the connection between the radial cracking systems [63, 64, 65, 66] is based on the phenomena related to the superimposition of the stress waves induced in the medium by a number of simultaneous or nearly simultaneous explosions.

#### 4.3 Influence of natural discontinuities on the propagation of radial cracks

The presence of natural discontinuities that cross the rock mass, and more generally, the dishomogeneity of the elastic characteristics of the medium influence the transmission of the stress wave induced in the rock mass by the explosion. The way in which the discontinuities influence the transmission of the stress wave is governed by the following relationship that relates the stresses to the elastic characteristics of the medium and by the continuity equation. This relationship applies to plane waves:

$$\sigma_T / \sigma_I = 2 / (1 + \rho_1 v_{r1} / \rho_2 v_{r2}) \quad (25)$$

$$\sigma_I + \sigma_R = \sigma_T \quad (26)$$

For the most interesting case in terms of radial crack extension, in which  $(\rho v_r)_2$  is smaller than  $(\rho v_r)_1$  (presence of fractures with or without fluid, or in two media where the modulus of elasticity  $E_2$  is smaller than  $E_1$ ),  $\sigma_T$  is smaller than  $\sigma_I$  and therefore for a  $\sigma_I$  of compression, a reflection stress wave in medium 1 is obtained.

The reflection processes are furthermore conditioned, for the case of joints, by the characteristics of the fluid that fills them

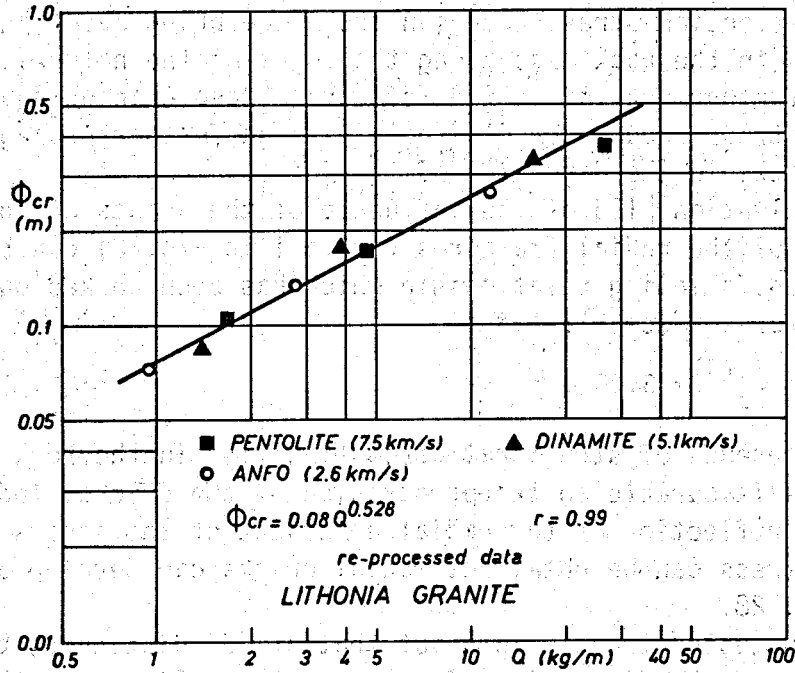


Fig.26 - Extension of the crushed zone versus the quantity of explosive contained in a 1-m hole. The experimental values [61] are based on explosions performed with different types of explosive and with decoupling between 1.2 and 1.26. The analysis of the results shows that the extension of the crushed zone appears to be independent from the explosive used

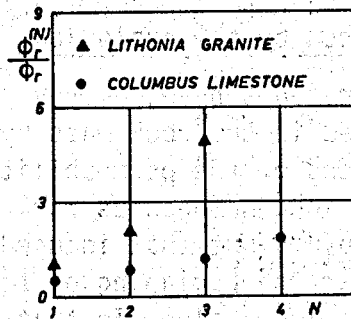


Fig.27 - Length of the radial cracks versus the number of explosions N carried out successively in the same blasthole. The explosions following the first one use explosion cavities that grow gradually larger proportionally with the diameter of the crushed zone produced by each previous explosion

and by those of the joints themselves.

The reflection stress wave can therefore bring about a further fracturing in the rock mass along the edges of the natural discontinuities; furthermore, since the reflection wave changes again the state of stress around the blasthole, it can further propagate the radial cracks in the direction of the joint.

An evaluation [11] of the influence of the joints on the maximum extension of the radial fractures (curve 1 in Fig.22) can be obtained through the following relationship which has been worked out from the one used for surface blasting:

$$\phi_r(d) = 3.28 Q^{0.5} \quad (27)$$

The presence of structural discontinuities in the rock mass is not always favourable to the propagation of the cracks. Indeed, if the total reflection of the radial component of the stress wave as tensile stress can be obtained, radial cracks can develop as indicated in Fig. 28.

The suggested trend points out that at "d" distances, between the blasthole and the discontinuities, that are smaller than the maximum radial extension of the cracks that can be obtained in a homogenous rock medium, the development of the fractures would be interrupted by the discontinuities. As the distance increases, the cracks propagate to a maximum value that can be approximately calculated by means of expression (27). For greater distances, the influence of the discontinuities decreases rapidly down to values where they are ineffective.

#### 4.4 Permeability induced by the explosion

Experimental measurements have, only very seldom, been made of the permeability induced in the rock mass by explosions.

The qualitative trend of the permeability induced by the explosion of cylindrical charges in a homogenous rock mass is illustrated in Fig. 29. The diagram points out that induced permeability is lower in the crushed zone than at the beginning of the radial fractured zone where it reaches its maximum value. In that latter zone it decreases gradually until it reaches the permeability values of the rock mass [66, 68, 69].

The loss of permeability in the radial fracturing zone can be expressed as a function of the distance from the axis of the blasthole



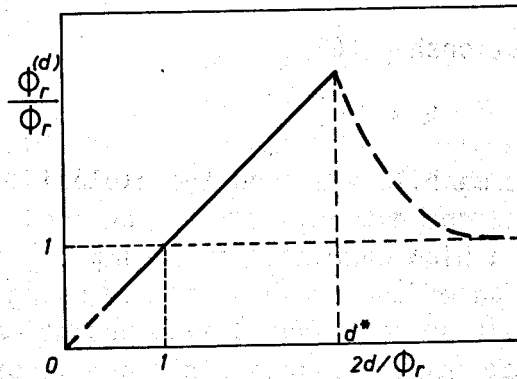


Fig.28 - Qualitative development of the radial cracks induced in a medium by structural discontinuities near the explosion cavity. The extension of the radial cracks induced by the explosion and influenced by the discontinuities ( $\phi_r^d$ ) is scaled from the extension that would be obtained under the same conditions in a homogeneous medium. If the discontinuity is near the hole, the radial fractures are interrupted by the joint and the value of  $\phi_r^d$  coincides with  $\underline{d}$ . As the joint-hole distance increases,  $\phi_r^d$  reaches a maximum value which is close to the critical distance. By further increasing the distance, the length decreases rapidly and it comes close to the values obtained for homogeneous rock masses

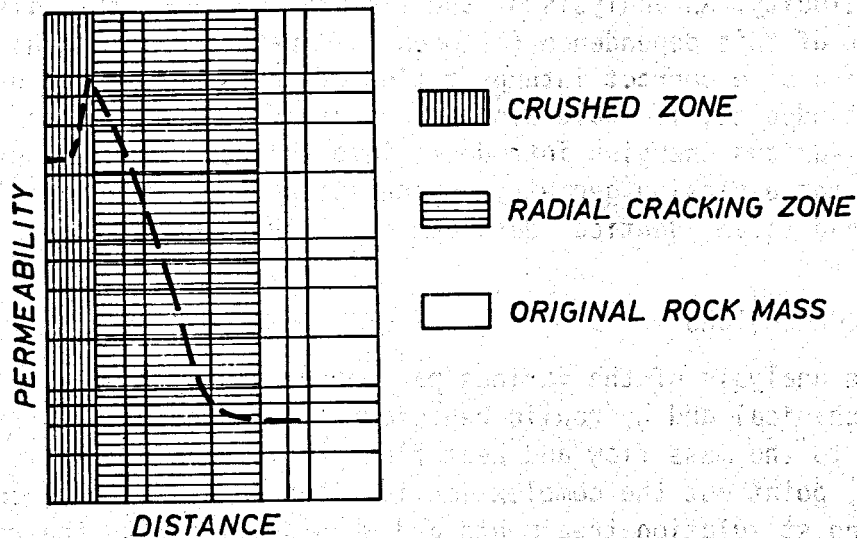


Fig.29 - Qualitative trend of the permeability induced by the explosions around a hole

by the following relationship [68]:

$$k \propto d^{-4} \quad (28)$$

An increase in permeability around the explosion cavity could be obtained by decreasing the extension of the crushed zone.

For rocks having a high characteristic impedance it is possible to reduce the extension of the crushed zone by using low detonation-rate explosives [54]; they do however, also produce a smaller radial cracking zone. In rocks having a less rigid behaviour, the extension of the crushed zone does not appear to be influenced by the type of explosive used [54].

If decoupling greater than one is used at a first approach, it can be stated that the development of the crushed zone does not appear to be influenced by the explosive used (Fig. 26) even in rocks having a high characteristic impedance. On the contrary, the stresses induced in the medium scaled by the extension of the crushed zone, vary with the explosive used. A detailed and complete analysis appears to be very complex for the time being. It can, however, be pointed out that the limits of the crushed zone are usually calculated by assuming that the induced dynamic stresses are equal to the dynamic strength of the medium. On the other hand it has already been emphasized that the strength varies considerably with the load rate (Fig. 5) and therefore also with the type of explosive and with the detonation velocity. An analysis of the failure phenomena that also keeps account of this dependence (between load rate and strength) could lead to a more correct interpretation of the experimental data. From this standpoint, it would also be necessary to analyse the influence of the various energies introduced into the medium by the explosives and by the explosion geometry on the extension of the radial cracks that lead to an identical development of the crushed zone.

## 5 - CONCLUSIONS

The analysis of the various parameters and of the laws that govern the mechanical and hydraulic behaviour of a geothermal reservoir in relation to the mass flow and heat flow problems and to stimulation processes, point out the complex implications that are involved when planning stimulation treatments and when dealing with the results obtained.

The models developed so far appear to be inadequate at large,

especially for Italian geothermal reservoirs that, in most cases, are structurally complex. Such drawbacks can be overcome by introducing into the mathematical model used, a greater number of parameters keeping account of the complexities of the reservoirs. This must be matched with more thorough and extensive theoretical and experimental research providing greater understanding of the events that are involved in the stimulation processes and that make the interpretation of the data obtained more reliable.

#### ACKNOWLEDGEMENTS

This research was partially financed by the National Research Council (CNR) of Italy (Contract n<sup>o</sup>. 79.01649.92).

#### REFERENCES

- | 1| Vakhitov G.G. et al.: "Selection of Efficient Methods Applied for the Increase in Well Productivity Based on the Probability and Statistic Models" - 10th World Petr.Congr., P.D.7, Bucharest, 1979
- | 2| Haimson B.C.: "Recent in Situ Stress Measurements Using the Hydrofracturing Technique" - 18th U.S.Symp.on Rock Mech., Keystone, Colorado, 1977
- | 3| Stagg K.G., Zienkiewicz O.C.: "Rock Mechanics in Engineering Practice" - pp. 55-97, Wiley and S., London, 1968
- | 4| Berry P. et al.: "The Influence of Fabric on the Deformability of Anisotropic Rocks" - 3rd Congr.of the ISRM, Vol. IIA, pp. 105-110, Denver, Colorado, 1974
- | 5| Brace W.F.: "Some New Measurements of Linear Compressibility of Rocks" - J.Geoph.Res., Vol. 70, pp. 391-398, 1965
- | 6| Walsh J.B.: "The Effect of Cracks on the Compressibility of Rock" J.Geoph.Res., Vol. 70, pp. 381-389, 1965
- | 7| Warren M.: "Theoretical Calculation of the Compressibility of Porous Media" - J.Geoph.Res., Vol. 78, pp. 352-362, 1973
- | 8| Geertsma J.: "The Effect of Fluid Pressure Decline on Volumetric Changes of Porous Rocks" - AIME Trans.SPE, Vol. 210, pp. 331-340, 1957
- | 9| Mann R.L., Fatt I.: "Effect of Pore Fluids on the Elastic Properties of Sandstone" - Geoph., Vol. XXV, n<sup>o</sup> 2, pp. 433-444, 1960
- | 10| Knutson C.F., Bohor B.F.: "Reservoir Rock Behaviour Under Moderate Confining Pressure" - 5th U.S.Symp.Rock Mech., Minnesota, 1963

- |11| Heard H.C.: "The Influence of Environment on the Brittle Failure of Rocks" - 8th U.S.Symp. Rock Mech., Minnesota, 1966
- |12| Logan J.M., Handin J.: "Triaxial Testing at Intermediate Strain Rates" - 12th U.S.Symp. Rock Mech., Rolla, Missouri, 1970
- |13| Perkins R.D. et al.: "Uniaxial Stress Behaviour of Porphyritic Tonalite at Strain Rates to  $10^3 \text{ s}^{-1}$ " - Int.J.Rock Mech.Min.Sci., Vol. 7, pp. 527-535, 1970
- |14| Stowe R.L., Ainsworth D.L.: "Effect of Rate of Loading on Strength" 10th U.S.Symp.Rock Mech., Austin, Texas, 1968
- |15| Schwartz A.E.: "Failure of Rock in the Triaxial Shear Test" - 1st Congr.ISRM, Vol. 1, pp. 109-151, Lisbon, 1966
- |16| Lehnoff T.F., Scheller J.D.: "The Influence of Temperature Depend Properties on Thermal Rock Fragmentation" - Int.J.Rock Mech.Min. Sci., Vol. 12, pp. 255-260, 1975
- |17| Clark K.K., Somerton W.H.: "Laboratory Investigation of Reduction of Fracture Pressures of Rocks by Intensive Borehole Heating" - AIME Trans.SPEJ, Vol. 234, pp. 225-228, 1965
- |18| Whitsitt N.F., Dysart G.R.: "The Effect of Temperature on Stimulation Design" - AIME Trans.SPE, Vol. 249, pp. 493-502, 1970
- |19| Hawle H. et al.: "Reservoir Geology of the Carbonate Oil and Gas Reservoir of the Vienna Basin" - 7th World Petr.Congr., Vol. 2, pp. 371-395, 1967
- |20| Wible D.O.: "Effect of Applied Pressure on the Conductivity, Porosity and Permeability of Sandstones" - AIME Trans.SPE, Vol.213, pp. 430-432, 1958
- |21| Perami R.: "Microfessuration of Rocks under Homogeneous Thermic Variations" - ISRM Symp.on Rock Fracture, Nancy, 1971
- |22| Le Tirant P., Baron G.: "Flow in Fissured Rocks and Effective Stresses.Application to Hydrocarbon Production" - ISRM Symp. Percolation through Fissured Rock, Stuttgart, 1972
- |23| Brace W.F. et al.: "Permeability of Granite under High Pressure" J.Geoph.Res., Vol. 73, pp. 2225-2236, 1968
- |24| Fisher H.N.: "Interpretation of the Pressure and Flow Date" - Proc.II NATO-CCMS Inf.Meet.on D.H.R.Geothermal Energy, Los Alamos, N.Mexico, 1977
- |25| Pomeroy C.D., Robinson D.J.: "The Effect of Applied Stresses on the Permeability of a Middle Rank Coal to Water" - Int.J.Rock Mech. Min.Sci., Vol. 4, pp. 329-343, 1967
- |26| Morgenstern N.R., Guther H.: "Seepage into a Extravation in a Medium Possessing Stress Dependent Permeability" - ISRM Symp.Percolation

- |27| Jouanna P.: "Laboratory Tests on the Permeability of Micaschist Samples under Applied Stress" - ISRM Symp. Percolation through Fissured Rock, Stuttgart, 1972
- |28| Mordecai M., Morris L.H.: "An Investigation into the Changes of Permeability Occurring in a Sandstone when Failed under Triaxial Stress Conditions" - 12th U.S. Symp. Rock Mech., Rolla, Missouri, 1970
- |29| Jager C.: "Rock Mechanics and Engineering" - Cambridge University Press, 1972
- |30| Potter J. "Laboratory Studies of Permeability" - Proc. II NATO - CCMS Inf. Meeting H.D.R. Geothermal Energy, Los Alamos, N. Mexico, 1977
- |31| Serafim J.L.: "Influence of Interstitial Water on the Behaviour of Rock Masses" - Rock Mechanics in Engineering Practice, Stagg K.G., Zienkiewicz O.C., Wiley J. and Sons, pp. 55-97, London, 1968
- |32| Baldi P. et al.: "Selection of Dry Wells in Tuscany for Stimulation Tests" - II Workshop for Coop. Res. in Geothermal Energy, Berkeley, California, 1980
- |33| Castillo E.: "Mathematical Model for Two-Dimensional Percolation through Fissured Rock" - ISRM Symp. Percolation through Fissured Rock, Stuttgart, 1972
- |34| Sharp J.C., Maini Y.N.T.: "Fundamental Considerations on the Hydraulic Characteristics of Joints in Rock" - ISRM Symp. Percolation through Fissured Rock, Stuttgart, 1972
- |35| Rayneav C., Jouanna P.: "Temperature Influence on Seepage through Fissured Media" - ISRM Rock Fracture, Nancy, 1971
- |36| Hubbert M.K., Willis D.G.: "Mechanics of Hydraulic Fracturing" - AIME Trans. SPE, Vol. 210, pp. 153-168, 1957
- |37| Kehle R.O.: "Determination of Tectonic Stresses through Analysis of Hydraulic Well Fracturing" - J. Geoph. Res., Vol. 69, p. 259, 1964
- |38| Haimson B.C., Fairhurst C.: "Initiation and Extension of Hydraulic Fractures in Rocks" - AIME Trans. SPE, Vol. 240, pp. 310-318, 1967
- |39| Daneshy A.A.: "Principles of Hydraulic Fracturing" - Proc. Symp. 103rd AIME Annual Meeting, Dallas, Texas, 1974
- |40| Timoshenko S., Goodier J.N.: "Théorie de l'élasticité" - Librairie polytechnique Ch. Béranger, Paris, 1961
- |41| Lubinski A.: "The Theory of Elasticity for Porous Bodies Displaying a Strong Pore Structure" - Proc. II U.S. N. Congr. Appl. mech., pp. 247-256, 1954
- |42| Murphy H.D.: "Thermal Stress Cracking and the Enhancement of Heat Extraction from Fractured Geothermal Reservoirs" - Informal Report

- LA-7235-MS, Los Alamos, N.Mexico, 1978
- [43] Wong H.Y., Farmer I.W.: "Hydrofracture Mechanisms in Rock During Pressure Grouting" - Rock Mech., Vol. 5, pp. 21-41, 1973
  - [44] Zoback M.D. et al.: "Laboratory Hydraulic Fracturing Experiments in Intact and Pre-Fractured Rock" - Int.J.Rock Mech.Min.Sci., Vol. 14, pp. 49-58, 1977
  - [45] Haimson B.C., Fairhurst C.: "In-Situ Stress Determination at Great Depth by Means of Hydraulic Fracturing" - 11th U.S.Symp.Rock Mech. Berkeley, California, 1969
  - [46] Von Schonfeldt H., Fairhurst C.: "Field Experiments on Hydraulic Fracturing" - AIME Trans.SPEJ, Vol. 249, pp. 69-77, 1970
  - [47] Haimson B.C.: "A Simple Method for Estimating in Situ Stresses at Great Depths" - 76th Annual Meeting ASTM, Philadelphia, 1973
  - [48] Haimson B.C., Avasthi J.M.: "Stress Measurements in Anisotropic Rock by Hydraulic Fracturing" - 15th U.S.Symp.Rock Mech., South Dakota School of Mines and Technology, 1973
  - [49] Berry P., Cataldi C.: "Geothermal well Stimulation at Torre Alfina" - ENEL-DSR, Relazione di Studio e Ricerca n° 355, 1978
  - [50] Abou-Sayer A.S.: "In Situ Stress Determination by Hydrofracturing: A Fracture Mechanics Approach" - J.Geoph.Res., Vol. 83, pp. 2851-2862, 1978
  - [51] Perkins T.K., Kern L.R.: "Widths of Hydraulic Fractures" - AIME Trans. SPE, Vol. 222, pp. 937-949, 1961
  - [52] Geertsma J., De Klerk F.: "A Rapid Method of Predicting Width and Extent of Hydraulically Induced Fractures" - AIME Trans.SPE, Vol. 246, pp. 1571-1581, 1969
  - [53] Le Tirant P., Dupuy M.: "Dimensions des fractures obtenie par fracturation hydraulique des couches pétroliferes" - Revue de l'Institute Français du Pétrole, Vol. XXII, n° 1, 1967
  - [54] Berry P. et al.: "Geothermal Stimulation with chemical Explosives" - Energy Technology Conference & Exhibition, Houston, Texas 1978
  - [55] Siskind D.E. et al.: "Fracturing in the Zone around a Blasthole" R.I. 7753, USEM, 1973
  - [56] Diadkin Y.D. et al.: "Theoretical and experimental Grounds for Utilization of Dry Rock Geothermal Resources in the Mining Industry" - 2° U.N.Symp.Dev.Use Geothermal Resources, S.Francisco, 1975
  - [57] D'Andrea D.V. et al.: "Crater Scaling in Granite for Small Charges" - R.I. 7409, USEM, 1970

- [58] Atchison T.C.: "Explosive Fragmentation Principles" - Abattage des roches a l'explosif - Rev. Industrie Minérale, num.spec., 1971
- [59] Nicholls H.R. et al.: "Comparative Studies of Explosives in Salt" R.I. 6041, USBM, 1962
- [60] Nicholls H.R. et al.: "Comparative Studies of Explosives in Granite" - R.I. 6693, USBM, 1965
- [61] Nicholls H.R. et al.: "Effect of Charge Diameter on Explosive Performance" - R.I. 6806, USBM, 1966
- [62] Atchison T.C. et al.: "Comparative Studies of Explosives in Limestone" R.I. 6395; USBM, 1964
- [63] Berry P. et al.: "Aumento della permeabilità di serbatoi geotermici mediante tecniche di stimolazione" - Energia Geotermica, I Seminario informativo, PEG, Roma, 1979
- [64] Weber P. et al.: "Calcul de la propagation d'une onde de contrainte à symétrie sphérique au cylindrique. Application au tir d'explosif" - Rev. Ind. Min., num.spec., 1971
- [65] Berry P. et al.: "Gli esplosivi nella coltivazione delle pietre ornamentali ed il controllo della fratturazione indotta" - Int. Days on the Quarrying Technologies of Ornamental Stones, Carrara, 1980
- [66] Mc Kee C.R. et al.: "Permeability from Single and Multiple Detonations of Explosive Charges" - Joint MMIJ-AIME Meet., Denver, 1976
- [67] Langefors U. et al.: "The Modern Technique of Rock Blasting" - Almquist and Wiksell, Stockholm, 1967
- [68] Schmidt R.A. et al.: "A New Perspective on Well Shooting. The Behaviour of Contained Explosions and Deflagrations" - 54th Annual Tech. Conf. Exh. SPE-AIME, Las Vegas, Nevada, 1979
- [69] Batchelor A.S. et al.: "Preliminary Studies of Dry Rock Geothermal Exploitation in Southwest England" - I.M.M., Vol. 88, Sect. B, pp. 51-56, 1979

## NOMENCLATURE

- $A_n$  = constants
- $B_c$  = blastability coefficient  $\sigma_{fd}/\sigma_{td}$
- $C_b$  = rock bulk compressibility
- $C_r$  = rock matrix compressibility
- $d$  = distance blasthole-discontinuity, distance
- $E_{sec}$  = Young Modulus (secant)

$E_{tg}$	= Young Modulus (tangent)
$e$	= opening fissure
$H$	= depth
$k$	= permeability
$k_0$	= initial permeability
$m$	= exponents
$N$	= number of explosions in the same hole
$n$	= porosity
$n_0$	= initial porosity
$P_0$	= initial pore fluid pressure
$P_w$	= borehole pressure
$p_w^C$	= $p_w^C - P_0$ critical borehole (break down) pressure
$Q$	= explosive quantity contained in a 1 metre length of the hole
$q$	= flow rate
$\bar{R}_1$	= $\phi(r, cr)/\phi_c$
$t$	= time
$T$	= temperature
$V_{cr}$	= crushed zone volume
$v_r$	= seismic velocity
$v_d$	= detonation velocity
$W$	= explosive quantity
$\alpha$	= $1 - C_r/C_b$ porous - elastic parameter of the rock
$\beta$	= linear thermal expansion coefficient
$\delta$	= charge density
$\epsilon_1$	= axial strain
$\dot{\epsilon}$	= strain rate
$\phi_{cr}$	= crushed zone diameter
$\phi_r$	= radial fracturing zone diameter
$\phi_r^{(d)}$	= radial fracturing zone in a medium by structural discontinuities
$\phi_r^{(N)}$	= radial fracturing zone diameter induced by a sequence of explosions in the same hole



- $\phi_c$  = equivalent diameter of TNT explosive charge  
 $\phi_h$  = blasthole diameter  
 $\rho_r$  = rock density  
 $\bar{\rho}_r$  = mean density of the overlying rock massif  
 $\sigma_{fd}$  = dynamic compressive strenght  
 $\sigma_f$  = compressive strenght  
 $\sigma_{td}$  = dynamic tensile strenght  
 $\sigma_t$  = tensile strenght  
 $\sigma'_{r,\theta,z}$  = principal effective stresses at the borehole wall  
 $\sigma'_{H1}$  = larger horizontal effective original stress  
 $\sigma'_{H2}$  = smaller horizontal effective original stress  
 $\sigma'_v$  = vertical effective original stress  
 $\bar{\sigma}', \bar{\sigma}$  = mean effective stress, mean state of total stress  
 $\sigma_I$  = incident stress wave  
 $\sigma_T$  = transmitted stress wave  
 $\sigma_R$  = reflected stress wave  
 $\sigma_1$  = major principal stress (axial)  
 $\sigma_3$  = minor principal stress (confining)  
 $\theta$  = angle measured counterclockwise from the radius in the direction of  $\sigma_{H1}$   
 $X_{(cr,r)}$  = dimensionless values  
 $\nu$  = Poisson's ratio